AD_____

GRANT NUMBER DAMD17-94-J-4464

TITLE: Construction and Characterization of Human Mammary Epithelial Cell Lines Containing Mutations in the p53 or BRCA1 Genes

PRINCIPAL INVESTIGATOR: Raymond L. White, Ph.D.

CONTRACTING ORGANIZATION: University of Utah
Salt Lake City, Utah 84102

REPORT DATE: January 1999

TYPE OF REPORT: Final

PREPARED FOR: Commander
U.S. Army Medical Research and Materiel Command
Fort Detrick, Frederick, Maryland 21702-5012

REPORT DOCUMENTATION PAGE

Form Approved
OMB No. 0704-0188

1. AGENCY USE ONLY *(Leave blank)*	2. REPORT DATE	3. REPORT TYPE AND DATES COVERED
	January 1999	Final (22 Sep 94 - 31 Dec 98)

4. TITLE AND SUBTITLE
Construction and Characterization of Human Mammary Epithelial Cell Lines Containing Mutations in the p53 or BRCA1 Genes

5. FUNDING NUMBERS
DAMD17-94-J-4464

6. AUTHOR(S)
Raymond L. White, Ph.D.

7. PERFORMING ORGANIZATION NAME(S) AND ADDRESS(ES)
University of Utah
Salt Lake City, Utah 84102

8. PERFORMING ORGANIZATION REPORT NUMBER

9. SPONSORING/MONITORING AGENCY NAME(S) AND ADDRESS(ES)
Commander
U.S. Army Medical Research and Materiel Command
Fort Detrick, Frederick, Maryland 21702-5012

10. SPONSORING/MONITORING AGENCY REPORT NUMBER

11. SUPPLEMENTARY NOTES
This report contains colored photos

12a. DISTRIBUTION / AVAILABILITY STATEMENT
Approved for public release; distribution unlimited

12b. DISTRIBUTION CODE

13. ABSTRACT *(Maximum 200*

The overall goal of this project is to identify and characterize the consequences of human mammary epithelial cells (HMEC) that become deficient in normal p53 or BRCA1 gene functions. We have created retroviral vectors which allow us conditionally express the E6/E7 gene of human papillomavirus type 16 (HPV16), dominant-negative p53 gene, or anti-sense BRCA-1 gene. The consequences of transduction of these viral constructs into primary human mammary epithelial cells will be discovered through controlled *in vitro* comparisons between genetically altered derivatives and their isogenic parent cells. As we proposed in our last report, we are now focused our efforts on microarray-based comparisons to identify breast cancer related genes. During the past year we have successfully implemented the Microarray Spotting and Scanning techniques. This includes development of robust fluorescent labeling and hybridization protocols as well as the preparation and testing of over 23,000 minimally redundant cDNA target samples for deposition on the microarray slides. We have compared expression profiles from several distinct breast cell lines we had created. We believe that this system will provide us critical information to our understanding of early breast carcinogenesis.

14. SUBJECT TERMS
Breast Cancer

15. NUMBER OF PAGES
59

16. PRICE CODE

17. SECURITY CLASSIFICATION OF REPORT	18. SECURITY CLASSIFICATION OF THIS PAGE	19. SECURITY CLASSIFICATION OF ABSTRACT	20. LIMITATION OF ABSTRACT
Unclassified	Unclassified	Unclassified	Unlimited

FOREWORD

Opinions, interpretations, conclusions and recommendations are those of the author and are not necessarily endorsed by the U.S. Army.

____ Where copyrighted material is quoted, permission has been obtained to use such material.

____ Where material from documents designated for limited distribution is quoted, permission has been obtained to use the material.

____ Citations of commercial organizations and trade names in this report do not constitute an official Department of Army endorsement or approval of the products or services of these organizations.

X In conducting research using animals, the investigator(s) adhered to the "Guide for the Care and Use of Laboratory Animals," prepared by the Committee on Care and use of Laboratory Animals of the Institute of Laboratory Resources, national Research Council (NIH Publication No. 86-23, Revised 1985).

NA For the protection of human subjects, the investigator(s) adhered to policies of applicable Federal Law 45 CFR 46.

X In conducting research utilizing recombinant DNA technology, the investigator(s) adhered to current guidelines promulgated by the National Institutes of Health.

X In the conduct of research utilizing recombinant DNA, the investigator(s) adhered to the NIH Guidelines for Research Involving Recombinant DNA Molecules.

X In the conduct of research involving hazardous organisms, the investigator(s) adhered to the CDC-NIH Guide for Biosafety in Microbiological and Biomedical Laboratories.

Ray White 1/29/99

PI - Signature Date

Table of Contents

(5) INTRODUCTION

Characterization of early events in the development of breast cancer is expected to bring a better understanding of how normal cells are transformed to malignancy and may suggest new strategies for detecting precancerous lesions and new treatment methods. Since germline mutations in two tumor suppressor genes, p53 and BRCA1, are associated with inherited predisposition to cancer (Malkin *et al.* 1990, Hall *et al.* 1990, Hollstein *et al.* 1991, Miki *et al.* 1994, Futreal *et al.* 1994), alterations in the p53 and BRCA1 genes represent some of the earliest genetic changes known to occur in the development of breast cancers. To study the effects of inactivating mutations in these tumor suppressor genes early in the breast-cancer pathway, we have originally proposed to create HMEC cell lines containing homologous deletions of p53 or BRCA-1 gene through gene targeting experiment. However, although our extensive screening, we were unable to establish such mutated cell line. As an alternative, we have created retroviral vector system stably or conditionally express the E6 and/or E7 gene of human papillomavirus type 16 (HPV16), dominant-negative p53 gene, and anti-sense BRCA1 gene, to study the effects of inactivating mutations in these tumor suppressor genes early in the breast-cancer pathway. The consequences of transduction of these constructs into primary human mammary epithelial cells were characterized through controlled *in vitro* comparisons between genetically altered derivatives and their isogenic parent cells. Recently our laboratory has gained access to this new technology through collaboration with Molecular Dynamics who has manufactured a small number of prototype microarray spotters and scanners for members of an early access program. Not only does this technique permit detection of the expression profiles of each of a large number of genes in parallel, but it potentially also provides a mechanistic view of how regulatory pathways are controlled in early breast carcinogenesis. Once candidate genes have been identified using this technology, they will be further characterized using conditional expression systems to assess changes in characteristics pertaining to morphology and growth rate.

(6) BODY

The following progress were made during the funded years

Task 1: Construction of human mammary epithelial cells (HMEC) containing mutations in the p53 or BRCA1 gemes.

Task 1a: Construct HMEC with altered activities of p53 and, when it is available, BRCA1.

Construction of HMEC deficient in p53.

We originally proposed three approaches for constructing p53-deficient cells; i.e., by mutating the p53 gene directly, by abrogating the protein's normal cellular function, or by introducing dominant negative p53 gene. Only the second and the third approach have been successful, and the reasoning is outlined below.

Approach #1: Construct HMEC containing homozygous deletions of p53 by homologous recombination.

The human *p53* gene, which is about 20 kb long, contains 11 exons and 10 introns (Appendices, Figure 1). Point mutations and small deletions have been found across the whole open reading frame, although hot spots cluster from exon 5 to exon 8. We have consrtucted knockout vectors (neoXBdt and neoPA(-)XBdt) which carry 12-kb homologous sequences that are disrupted

by a neo gene and flanked by two copies of the *tk* gene (Figure 1). A 4-kb DNA fragment covering a small portion of the huge intron 1, the whole exon 2 which contains the translation start codon, and part of intron 2 was deleted and replaced by a 2.67-kb complete neo gene cassette or a 1.25-kb neoPA(-) gene cassette.

Homologous recombination of the *p53* gene should yield a 10 kb (neoXBdt, neoXBP) or 8.6 kb (neoPA(-)XBdt) knockout allele in an XbaI digest, while the wildtype allele should give rise to a 10.6-kb band when a SmaI-XbaI DNA fragment from exon 11 is used as a probe. With an XbaI-EcoRI DNA fragment from exon 1 and intron 1 as the probe, a 7.5-kb knockout allele and a 11.2-kb wildtype allele should be detected in BamHI-digested genomic DNA from clones of heterozygous knockout cells.

Two transfection methods, calcium phosphate co-precipitation and lipofection, were tested in immortalized HMEC, 184A1 cells (Stampfer *et al.* 1985). Among several commercially available lipofection reagents, DOTAP (Boehringer Mannheim) showed best efficiency. Different ratios of DNA:DOTAP are known to affect transfection efficiency and should be optimized for each cell type. By fixing the amount of DOTAP (30μl) and changing the amount of DNA (linearized) from 1 to 10 μg, we found that toxicity to cells increased as the amount of DNA increased and that 5 μg DNA gave rise to more stable transformants (~15 colonies from 5 x 10^5 cells).

Positive selection with G418 and negative selection with ganciclovir are frequently used to select cell clones that have undergone homologous recombination. The optimal concentration of ganciclovir (2 μM) for negative *tk* gene selection in embryonic stem (ES) cells has been worked out by Mansour *et al.* (1988). To test the optimal ganciclovir concentration for negative selection in HMEC, we first introduced a neo*tk*/SK+ vector into the 184A1 cell line. Stable transformants were selected with 200 μg/ml G418. As shown in Figure 2, 184A1 cells expressing the HSV-*tk* gene (neo*tk*/184A1) are more resistant to ganciclovir. Cell growth of neo*tk*/184A1 was not much affected at concentrations lower than 2 μM, and dropped dramatically only when up to 20 μM ganciclovir was used. At this concentration (20 μM), the growth of parental 184A1 cells was only slightly inhibited. Thereafter we used MCDB 170 or DFCI-1 complete medium containing 200 μg/ml G418 and 25 μM ganciclovir routinely for positive and negative selection in 184A1 cells. However, the enrichment factor of ganciclovir selection in 184A1 cells was only 1.5-2.0. A polyadenylation trap positive selection provided another 3- to 4-fold enrichment (neoPA(-)XBdt vs. NeoXBdt, data not shown).

Forty four clones from neoXBP transfection, 171 clones from neoXBdt transfection, and 120 clones from neoPA(-)XBdt transfection were obtained and subjected to Southern analysis. However, none of these 335 clones carried the knockout allele. Apparently, the frequency of homologous recombination is very low in 184A1 cells. One possible explanation for this low frequency of homologous recombination is the sequence mismatches between targeting vector and the recipient DNA due to polymorphisms.

Approach #2: Construct p53-deficient HMEC by introduction of human papillomavirus type 16 E6.

Interactions between the tumor supressor proteins p53 and Rb and transforming proteins of various DNA tumor viruses are thought to be essential components of the transformation process. The E6 and E7 proteins encoded by human papillomavirus type 16 (HPV16) bind and inactivate p53 and Rb proteins, respectively (Dyson *et al.* 1989, Scheffner *et al.* 1990, Werness *et al.* 1991).

Binding of HPV16 E6 to p53 enhances degradation of the p53 protein, whereas binding of HPV16 E7 to Rb inactivates Rb by mimicking the hyperphosphorylated state, and thereby disrupting phosphorylated Rb interactions with other proteins. Thus, E6 and E7 effectively delete p53 and Rb without actually knocking out these genes. However, it should be noted that p53 and Rb are not only proteins to bind to HPV16 E6 and E7. Carefully controlled experiments are necessary. Such experiments include analyses with an array of HPV16 E6 and E7 mutants that exhibit differential ability to abrogate p53 and Rb functions.

From Dr. D. A. Galloway, Fred Hutchinson Cancer Research Center, Seattle), we have obtained PA317 amphotropic packaging cell lines that express LXSN-based retroviral vectors (Miller *et al.* 1989, 1993) containing HPV16 E6 and/orE6 (Halbert *et al.* 1991). The viral supernatant from each packaging line, filtered through a 0.45-micron disposable syringe filter, was used for infections. Many of our HMEC cultures have been successfully transduced with E6 and/or E7 genes. We have confirmed the absence of p53 protein in E6-transduced HMEC by Western analysis (data not shown).

Approach #3: Construct p53-deficient HMEC by introduction of dominant negative mutant p53 gene.

The p53 protein functions as a sequence-specific DNA binding protein and, thereby, acts as a transcriptional activator (Kern 1994). Following the exposure of cells to agents that induce DNA damage, the levels of p53 protein increase, resulting in increased transcription of genes that carry a p53 binding site, such as GADD45, mdm-2, WAF1, cycline G, BAX, and insulin-like growth factor binding protein-3 (Cao 1997). It is thought that oncogenic p53 mutations either abrogate DNA-binding or induce conformational changes that alter the transcriptional activation. Indeed, the vast majority of cancer associated mutations reside within the DNA-binding domain of p53 (Cao 1997). As p53 protein binds to DNA as a tetramer, it is thought that mutant p53 proteins oligomerize with the wild-type p53 and drive it in to a mutant, presumably inactive, conformation, accounting for dominant negative inhibitory phenotype. Recently, Dr. V. Band's group at Tufts University have shown that retrovirus mediated expression of two hot-spot p53 mutants (del239, R248W) induce dominant immortalization of normal primary HMEC (Cao et al. 1997). We have obtained these dominant negative p53 retroviral constructs (in collaboration with Dr. V. Band) and successfully transduced into and immortalized our HMEC.

Construction of HMEC deficient in BRCA1.

Our original proposal to construct BRCA1-deficient HMEC by homologous recombination has been unsuccessful for the same reason described in p53 knockout experiments. Our attempt to down-regulate BRCA1 expression by addition of a BRCA1 antisense oligonucleotide (Thompson et al. 1995) to the growth medium was not effective (data not shown). As an alternative, we have found it necessary to implement a more sensitive, reliable anti-sense or dominant negative gene expression system, preferably using a conditional expression system (described in Task 2b).

Task 1b: Develop cell strains from individuals carrying constitutional mutations in their p53 or BRCA1 genes and select cells that are homozygous for the mutant alleles.

We originally proposed to develop HMEC lines that are already heterozygous for mutant alleles by culturing breast biopsies from individuals who are known carriers of tumor suppressor gene mutations. We have established over 200 primary HMEC cultures from breast tissue specimens, many of them from women who carry abnormal alleles of the BRCA1, BRCA2, APC, or NF1 genes (Table 1). Daughter cell lines that have lost the remaining wild-type allele, therefore become homozygous for mutated allele, would be selected for *in vitro* mitotic nondisjunction

events. As an initial test, we have treated HMEC carring a known mutation of APC gene, with vinblastine and vincristine, inhibitors of microtuble assembly. The outgrowing clones of treated cells were isolated and were screened for the loss of wild-type allele by nondisjunction event, using a PCR-based fluorescence genotyping. Out of 36 clones isolated, 4 clones underwent for nondisjunction for APC allele, however, unfortunately all of them retained only the wild-type alleles (data not shown). At present we do not know whether "selection" existed against mutated APC allele during nondisjunction event. We are currently screening for nondisjuction on HMEC allele carrying a BRCA1 mutation.

Task 2: Characterization of HMEC containing mutations in the p53 or BRCA1 genes.

Task 2a: Characterize the cell lines with altered activities of p53 or BRCA1, with respect to their growth properties and behavior.

Telomerase activation.

Although common in rodent cells, spontaneous escape from senescence *in vitro* and the acquisition of an indefinite lifespan is an exceptionally rare event in human cells (Linder *et al.* 1990, Shay *et al.* 1989, 1991). The ability of the E6 and E7 genes of human papillomavirus type 16 (HPV16), which target p53 and Rb functions respectively, to immortalize human fibroblasts, keratinocytes, uroepithelial cells, and mammary epithelial cells has provided a useful model for studying the transformation process. However, as not all cell types are immortalized by HPV16 E6 and E7 with the same efficiency (Hawley-Nelson *et al.* 1989, Munger *et al.* 1989, Band *et al.* 1991, Halbert *et al.* 1991, Shay *et al.* 1991, Reznikoff *et al.* 1994), the growth control pathways targeted by HPV16 E6 and E7 appear to differ among cell types.

Cultures of human mammary epithelial cells (HMEC) derived from mammoplasty tissues show two distinct phases of growth. The cultures proliferate aggressively for several passages and consist primarily of cells with ductal characteristics. This is followed by a period called 'selection' (Stampfer 1980) or 'mortality stage 0 (M0)' (Foster 1996) when the majority of the cells become larger, flattened, and nonproliferative (Stampfer 1980, Hammond 1984). However, held in culture with continued feeding, a population of small cells of indeterminate phenotype often emerges and proliferates for another 10-20 passages before senescence (Stampfer 1980, Hammond 1984). These cells show decreased expression of cyclin-dependent kinase inhibitor p16 due to silencing of the gene (Foster 1998).

Previous studies have suggested that HMEC at the different stages are immortalized with different efficiencies by the HPV-16 E6 and E7 genes. However, the observations and interpretations vary among studies. Wazer *et al.* (1995) have shown that early-passage (pre-selection) HMEC were immortalized readily by E7, but rarely by E6. Late-passage (post-selection) HMEC were immortalized efficiently by E6, but not E7, suggesting that early- and late-passage HMEC contain cell populations that differ with respect to E6 and E7 sensitivity. Foster *et al.* (1997), on the other hand, observed that early-passage (pre-G0) HMEC were immortalized by E6, but not E7. A more recent study (Kiyono *et al.* 1998) indicates that E6 is able to immortalize HMEC in late-passage (post-M0), but not in early-passage (pre-M0), while E7 had no effect on either.

While the mechanism that controls the timing of cellular senescence and immortalization remains unknown, increasing evidence (Morin 1989, Greider 1990, Hastie *et al.* 1990, Harley 1991, Blackburn 1991, 1992, Allsopp *et al.* 1992, Kipling *et al.* 1992, Levy *et al.* 1992) suggests that sequences at the ends of chromosomes (telomeres) act as molecular clocks. Telomeres, composed of

TTAGGG repeats, become shorter as a function of aging *in vivo* (Allsopp *et al.* 1992, Hastie *et al.* 1990) and during the passage of normal cells *in vitro* (Counter *et al.* 1992, Harley *et al.* 1990). This loss of telomeric DNA is thought to contribute to senescence (Levy *et al.* 1992, Harley 1991). Activation of a mechanism to restore telomeres, namely telomerase activation, has been proposed as a critical event in the immortalization of human cells (Morin 1989, Greider 1990, Hastie *et al.* 1990, Harley 1991, Blackburn 1991, 1992, Allsopp *et al.* 1992, Kipling *et al.* 1992, Levy *et al.* 1992). We chose to examine HMEC at different stages that were expressing HPV16 E6 and E7 together or separately from retroviral constructs (Halbert *et al.* 1991), with a view to establishing a temporal relationship between expression of different oncogenes, immortalization of different cell types, and activation of telomerase.

Different susceptibilities of early- and late- passage HMEC for immortalization to HPV16 E6 and E7 genes.

We introduced the HPV16 E6 and E7 genes, separately or in combination, into early-passage (initial outgrowth) and late-passage (post-selection) HMEC by retroviral infection, using the same viral titers and the same numbers of recipient cells. Following viral infection, cells were cultured in DFCI-1 medium containing 25 μg/ml G418 and examined for senescence, extension of life span, crisis, or immortalization. Despite the use of a different medium, our results were quite similar to those of Wazer *et al.* (1995) who used D2 medium which selects for outgrowth of immortal cells. E6 immortalized our late-passage HMEC very efficiently with a minimal (~1 week) crisis period, whereas E6-transduced early-passage HMEC gave rise to few immortal clones. In contrast, E7 was incapable of immortalizing late-passage HMEC, but E7-transduced early-passage HMEC resulted in a rapidly growing cell population, followed by a crisis period (4 weeks). Although many cells senesced during this crisis period, growing cells that emerged have been in culture for more than 70 passages. The combination of E6 and E7 led to a population of rapidly growing cells with a minimal (~1 week) crisis period, followed by efficient immortalization in both early-passage and late-passage HMEC.

Cell type-specific activation of telomerase by E6 and E7 in pre-crisis HMEC.

We examined telomerase activity in pre- and post-crisis HMEC using a modified version of the telomere-repeat amplification protocol (TRAP) assay. As shown in Fig. 3, those cells which became immortal (E7- and E6E7-transduced early-passage HMEC and E6- and E6E7-transduced late-passage HMEC) exhibited a high level of telomerase activity. Surprisingly, we have also detected telomerase activity at passage 4 after retrovirus infection when those cells were still in pre-crisis, that is, before immortalization. Cells transduced with vector control remained negative for telomerase activity. (Figure 3). Serial dilution of cell extracts and a subsequent TRAP assay indicated that telomerase activity in pre-crisis cells was 5-15% of the level in each corresponding population of post-crisis immortal cells (data not shown).

Telomerase is activated within one passage of retroviral infection.

To determine how soon telomerase is activated after introduction of HPV oncogenes, we performed TRAP assays of early-passage and late-passage HMEC within 1 passage of high-titer retrovirus infection. As shown in Figure 4, telomerase activity was detected in early-passage HMEC transduced with E7 alone, or with E6 and E7 together, as early as 2 days after infection. On the other hand, telomerase activity was detected within 2 days in late-passage HMEC transduced with E6 alone or with E6 and E7 together. Specificity of telomerase activation for cell type became more evident 8 days after infection. Transduction of the vector control did not activate telomerase in

either cell type. However, it should be noted that in early-passage HMEC transduced with E6 alone, and in late-passage HMEC transduced with E7 alone, small but detectable amounts of telomerase activity were induced after high-titer infection of retroviruses.

These results suggest that cell type-specific telomerase activation occurred soon after the introduction of viral oncogenes, and was not due to a rare genetic event in a given cell population.

Clonal analysis of pre-crisis HMEC for telomerase activity, immortalization, and senescence.

To determine whether any differences in telomerase activity exist among the cells of a pre-crisis population, we isolated sixteen clones from E7-transduced HMEC^{E} (see Materials and Methods). The levels of telomerase differed widely among the clones as shown in Figure 5. As the cells underwent the next several passages, the majority of progeny cells from each subclone were seen to senesce and die (clones S1-S12). However, four of the sixteen clones did yield immortalized cultures (clones Im1-Im4). Interestingly, the level of telomerase activity of each clone at pre-crisis also varied widely among both the four clones that yielded immortalized progeny as well as among the twelve clones that only senesced (Figure 5). Indeed, some senescent-only clones (clones S4, S5, S8, and S10) expressed much higher levels of telomerase activity than clones which yielded immortalized progeny, suggesting that the level of telomerase activation at pre-crisis is not critical in determining the probability of generating immortalized progeny. Furthermore, although the level of telomerase activity increased approximately ten-fold following immortalization in clones Im1 and Im3 (Figure 3), the level of telomerase remained relatively low (in clone Im2), or even decreased upon immortalization (in clone Im4). These results clearly indicate that telomerase activation does not directly condition the probability of immortalization for these cells.

To examine whether telomere shortening controls the timing of cellular senescence, we determined telomere length on DNA samples from E7-transduced HMEC^{E} at passage 1 and at crisis and from E7-immortalized clones (Im1-4). As shown in Figure 6, between passage 1 and crisis, the average telomere length decreased from approximately 9 to 6.5 kb in spite of the presence of telomerase activity. More importantly, all four immortalized clones showed, after 30 passages, an even shorter average telomere length (4.5-5.5 kb) than mixed populations of cells at crisis, suggesting that telomere shortening observed before crisis does not directly contribute to the timing of senescence. Interestingly, immortalized clones Im1 and Im3, which had high telomerase activity (Figure 5), showed shorter telomere length than other two clones.

Do these observations reflect the ability of E7 and E6 to target Rb and p53 functions? E7 protein associates with Rb and interferes with its binding to E2F, resulting in impaired Rb cell cycle control functions (Weinberg 1996). As shown in Figure 7B, expression of E2F-1 protein in HMEC^{E} induces telomerase activity, but not immortalization (data not shown), supporting the idea that the relevant target of the E7 protein with respect to telomerase activation is the underlying E7-Rb-E2F pathway. Recently, Jiang et al. (1998) had shown that Myc induces telomerase in both normal HMEC and fibroblasts. Myc is one of the target genes activated by E2F. Interestingly, our HMEC^{E} transduced with E7, E6/E7 and E2F-1 exhibited the increased levels of c-Myc protein and E6 had no effect (Figure 7C), suggesting the possible participation of c-Myc in activating telomerase in these cells.

In order to clarify the possible role of E7-Rb-E2F pathway as mechanisms for telomerase activation and immortalization, experiments with the mutant forms of E7 lacking in its ability to bind to Rb and related proteins would be necessary. On the other hand, regarding to telomerase

activation by E6, Klingelhutz *et al.* (1996) have shown that mutations in E6 that abrogate its ability to target p53 for degradation do not affect telomerase activation in keratinocytes, suggesting a p53-independent pathway.

E7-transduced HMEC^{E} thus express high levels of pre-crisis telomerase activity, more than ten-fold greater than that expressed by the E6-transduced HMEC^{E} (Figure 4) and E7 readily immortalized HMEC^{E} whereas E6 immortaled HMEC^{L}, similar to the previous observation of Wazer *et al.* (1995). In contrast, Klingelhutz *et al.* (1997), Stöppler *et al.* (1997), and Kiyono *et al.* (1997) reported that while transduction of HPV-16 E6 into early-passage HMEC induced pre-crisis activation of telomerase, transduction of E7 had no effect. Similarly, Foster *et al.* (1997) reported that HMEC^{E} (pre-M0) were immortalized by E6, but not E7. More recently, Kiyono *et al.* (1998) have reported E6 is able to immortalize HMEC^{L} (post-M0), but not HMEC^{E} (pre-M0), while E7 had no effect on cells from either culture stage. We do not at present understand the basis for these differences for telomerase activation and immortalization in response to E6 and E7 genes. Interestingly, Wazer *et al.* (1995) used DFCI-1 medium and then shifted the cultures to D2 medium to select for immortal cells, whereas we and others (Foster 1998, Kiyono 1998) kept cultures in DFCI-1 medium, yet our result for immortalization assay was basically identical to the report of Wazer et *al.* (1995). It is possible that differences in the preparation of breast organoids or the supplements for DFCI-1 medium (i.e. serum and bovine pituitary extracts) are responsible.

In summary, we have shown that the HPV16 E6 and E7 oncogenes can each induce telomerase and support immortalization of human mammary epithelial cells in culture. The majority population present in initial-outgrowth has a relatively short life span and is responsive to the HPV E7 oncogene, but not E6, with respect to telomerase induction and immortalization. The cell population which overtakes the culture following the selection phase, however, is responsive only to E6. In each immortalization pathway, telomerase induction follows very shortly upon introduction of the oncogene, substantially preceding the immortalization step. That each oncogene induces both telomerase activity and immortalization potential would suggest that the two are coupled and that telomerase induction might be a normal prerequisite to immortalization. Indeed, the finding that almost all tumors and immortalized cell lines are induced for telomerase would strongly support this view. It should be noted, however, that these cells, induced for telomerase, are not directly immortalized but will still go through a crisis phase from which only a small number of cells will survive to found an immortal culture. This implies that additional genetic changes may be required for immortalization.

Furthermore, the finding that some clones which did not yield immortalized progeny expressed higher telomerase activity than other clones which yielded immortalized progeny, suggests that the level of telomerase activation is not critical in determining the probability of generating immortalized progeny. Indeed, although the level of telomerase activity increased approximately ten-fold following immortalization in some clones, it remained relatively low, or even decreased, in others (Figure 5). In addition, the immortalized clones had a shorter average telomere length compared to cells at crisis period when the majority of cells failed to become immortal, suggesting that telomere shortening does not directly control the timing of cellular senescence. Similarly, the expression of E2F-1 induced telomerase activity and c-Myc in initial-outgrowth HMEC but was not sufficient to promote immortalization. This indicates not only that the mechanism underlying telomerase activation by E7 is partly mediated by E2F-1, but that E7 provides an additional component necessary for immortalization. One possibility is that telomerase induction is not a prerequisite for immortalization for these cells. Increasing number of evidences

suggests that telomerase activation is not always the sole mechanism controlling the timing of cellular senescence and immortalization. For example, expression of the catalytic component of telomerase (hTERT) is enough to immortalize primary human fibloblasts, but not keratinocytes or HMEC (Kiyono 1998, Morales 1999). Additional mechanisms, such as inactivation of Rb function by E7 or an decrease in cyclin-dependent kinase inhibitor p16, have been proposed (Kiyono 1998, Foster 1998). What our telomerase expressing E7-HMEC^{E} still go through crisis period before being immortalized, however, is that further mechanism is required in addition to telomerase activation and Rb/p16 inactivation by E7 to create the immortalization potential that we see here in the HMEC^{E}.

Insensitivity to growth inhibition by TGF-β.

Transforming growth factor β (TGF-β) inhibits growth of normal breast epithelial cells but dose not effect the proliferation of some of breast cancer cells (Hosobuchi *et al.* 1989). The loss of TGF-β response is thought to be an indicator of transformation and potentially could be a marker in the carcinogenecis pathway. Earlier studies with primary HMEC cell line (184) and immortalized HMEC cell line (184A1) showed full growth inhibition of 184 cells by TGF-β at 3.0 ng/ml, while 184A1 cells had varying levels of incomplete inhibition (10-30% of normal growth) (Hosobuchi *et al.* 1989). These results suggested that immortalized cells, such as those containing HPV16 E6 and/or E7, would have a different TGF-β growth response than the normal parental cells. Our preliminary results indicate that growth of late-passage HMEC immortalized with E6 and E6E7 is not inhibited by TGF-β , a characteristic not attributed to normal cells, suggesting that these cells may represent a stage along the carcinogenetic pathway. We are now performing a more detailed analysis of TGF-β sensitivity using various combinations of early- and late-passage HMEC and HPV16 E6 and E7 genes.

Isolation of pure populations of luminal and basal epithelial cells from human mammary gland.

Most breast cancers arise from epithelial cells of the mammary gland. Two types of epithelial cells are most common in the mammary gland: a continuous layer of glandular cells (luminal cells) lines the duct, whereas a discontinuous layer of cells near the basement membrane (basal cells) shares certain features of myoepithelial cells (Taylor-Papadimitriou *et al.* 1987). Intermediate phenotypes have also been observed. Basal cells predominantly express 5 types of keratins (K), K5, K6, K7, K14, and K17, whereas luminal cells predominantly express 3 types, K8, K18, and K19 (Taylor-Papadimitriou *et al.* 1987, Trask *et al.* 1990, Bartek *et al.* 1991). Breast-cancer cells produce mainly K8, K18, and K19 (Trask *et al.* 1990). In order to characterize more details of breast cell types in regard to the experiments described above, we have established a system for isolating pure populations of luminal and basal epithelial cells from human mammary gland. Briefly, monoclonal antibodies specific to surface antigens of either luminal or basal cells were bound to magnetic microspheres coated with a second antibody. These specific antibody/bead complex were then used to directly isolate purified luminal or basal cells from human breast organoid cell preparations by magnetic separation (Gomm *et al.* 1995, O'Hare *et al.* 1991). We are now testing these pure populations of luminal and basal epithelial cells to establish temporal relationships among features such as expression of HPV16 E6 and E7, p53 and Rb functions, immortalization, TGF-β sensitivity, response to *bcl-2* overexpression, and activation of telomerase.

Characterization of HMEC deficient in p53 and BRCA1 by structure formation in Matrigel.

The consequences of mutations in regulatory genes like p53 and BRCA1 genes should be associated with observable cellular and molecular changes. Bisssell et al. have shown that culturing breast epithelial cells in an extracellular matrix Matrigel provides a functionally relevant microenvironment conductive to form three-dimensional structures collagen (Weaver et al. 1996, Weaver et al. 1997). Normal cells will form differentiated spheroids with a central lumen. These structures express certain cell lineage markers such as sialomucin at the apical membrane and type IV collagen at the basal membrane. Breast cancer cells, however, are disorganized and lack polarized expression of these markers (Weaver et al. 1996, Weaver et al. 1997). In collaboration with the Bissell laboratory, we have established three-dimensional culture system in our laboratory.

Normal HMEC were infected with a retroviral vector expressing HPV16 E6 and/orE7. These infected cells, as well as the parental HMEC were embedded in the extracellular matrix Matrigel and cultured over a twenty day period. Immunostaining for many markers including cytokeratin 19, lactoferrin, type IV collagen, and E-cadherin were performed on frozen sections as described in Materials and Methods.

Structure formation of HMEC-E7 in Matrigel

E7 transduced HMEC formed spheroids morphologically identical to the normal, parental structures. Figure 14 shows a phase contrast image of a structually normal-appearing HMEC-E7 spheroid. Since the HMEC-E7 were forming morphologically normal structures, we were interested in further characterizing the shpheroids in regard to the markers described above.

E-cadherin and type IV collagen expression in HMEC-E7 spheroids.

HMEC-E7 cultures showed a normal staining pattern for E-cadherin and type IV collagen (Figure 15). E-cadherin is a cell-cell adhesion marker and showed a lateral localization pattern at points of cell-cell contact in both the normal HMEC and HMEC-E7 (Figure 15). Additionally, both cell cultures basally deposited a continuous type IV collagen-containing basement membrane (Figure 15).

Lactoferrin and cytokeratin expression in HMEC-E7 spheroids.

Immounohistochemistry for lactoferrin and cytokeratin 19 proteins was performed on frozed sections as described in Materials and Methods. Most normal HMEC spheroids expresssed both the iron-binding milk protein lactoferrin and the luminal differentiation marker cytokeratin 19 (Figure 16 A and B, respectively). The HMEC-E7 spheroids, however, do not express lactoferrin or cytokeratin 19 (Figure 16).

Structure formation of HMEC-E6 and HMEC-E6E7 in Matrigel

Interestingly, HMEC-E6 did not form structures when cultured in Matrigel. However, HMEC expressing both E6 and E7 formed formed spheroids morphologically identical to the normal, parental structures (data not shown). HMEC-E6 remained as single cells with condensed cytoplasm and surface blebbing, typical of cells undergoing apoptosis. We are currently determining if these cells are dying via apoptosis. HMEC-E6E7, however, formed normal-appearing spheroid structures (data not shown). This data suggests that inactivation of pRB by E7 might compensate the p53 deficiency in HMEC-E6E7, allowing for proper structure formation. This drastic difference in HMEC-E6 and HMEC-E6E7 could be due to difference in the expression of proteins involved in extracellular signaling pathways, a hypothesis currently investigation. Additionally, variations in other types of gene expression could also account for the behavioral changes. We are currently using microarray technology to determine variations in mRNA expression in our different HMEC cultures (described below).

Task 2b: Determine whether HMEC can be immortalized by induction of tsA58 (the temperature-sensitive allele of SV40 T-antigen), a conditionally expressed HPV16 E6 gene, or a conditionally expressed bcl-2 gene.

Induction of tsA58 (the temperature sensitive allele of SV40 T-antigen)

We have obtained retroviral construct expressing tsA58 from Dr. P Jat. This construct has been successfully used to conditionally immortalize various primary cultures derived from rodent tissues. However, unlike E6 and/or E7 genes, tsA58-transduced HMEC (both in early- and late-passages) failed to become immortal at the effective temperature, consistent with the observation of Dr. P. Jat (personal communication).

Overexpression of bcl-2 in immortalized HMEC, 184A1.

Bcl-2, a protooncogene originally found in follicular lymphoma (Bakhshi *et al.* 1985), can prevent the programmed cell death (apoptosis) induced by withdrawal of growth factor in lymphocytes (Hockenbery *et al.* 1990, Deng *et al.* 1993) and neurons (Allsopp *et al.* 1993), or by serum deprivation in fibroblasts overexpressing *c-myc* (Bissonnette *et al.* 1992, Fanidi *et al.* 1992). This suggests that overexpression of *bcl-2* may be able to protect HMECs from programmed cell death and may contribute to the immortalization of HMECs.

We transfected 181A1 cells with bcl-2 overexpression vector, pCMVhubcl-2-neo (Figure 7), and characterized three stable clones (4-1, 4-2 and 4-3). The *bcl-2* gene has three transcripts (8.5, 5.5 and 3.5 kb) in lymphocytes (Tsujimoto *et al.* 1986). No endogenous *bcl-2* mRNA was detected in 184A1 cells with a *bcl-2* DNA probe. A ~3 kb exogenous *bcl-2* mRNA was detected in clones 4-1 and 4-2, but not in 4-3 (Figure 8). Consistent with results of Northern analysis, Western blots analysis showed that the 26-kd Bcl-2 protein was barely detectable in either the parental 184A1 cells or the 4-3 clone, and was expressed at high levels in the 4-1 and 4-2 clones (Figure 8). Both 184A1 and clone 4-3 were used as negative controls for characterization of the *bcl-2*-expressing clones, 4-1 and 4-2.

Overexpression of *bcl-2* inhibits apoptosis in a variety of cell types, including lymphocytes, neurons, and fibroblasts (Hockenbery *et al.* 1990, Deng *et al.* 1993, Allsopp *et al.* 1993, Bissonnette *et al.* 1992, Fanidi *et al.* 1992). We first checked whether overexpression of *bcl-2* could protect 184A1 cells from 5-FUdR-induced apoptosis. As shown in Figure 9, after 4-day treatment with 100 μM 5-FUdR ~50% of the 184A1 and 4-3 cells had died, while only ~20 % of 4-1 or 4-2 cells died of the treatment. Therefore, overexpression of *bcl-2* conferred 2.5-fold protection from 5-FUdR-induced cell death. Degradation of genomic DNA was taken as evidence of cell death by apoptosis. DNA fragmentation analysis was carried out in clones 4-2 and 4-3 (Figure 10). Fragmented DNA was detectable by agarose gel electrophoresis analysis within the first 24 hours in 4-3, and increased within the following 24 hours of 5-FUdR treatment. In 4-2, no DNA fragmentation was observed within the first 24 hours of 5-FUdR treatment. It was detected within 48 hours, but was much less extensive than in 4-3. Thus DNA fragmentation was delayed in *bcl-2*- overexpressing clone (4-2) compared to the clone (4-3) which did not express exogenous *bcl-2*. Altogether, these data indicate that HMEC 184A1, like other cell types, are protected from induced apoptosis by overexpression of *bcl-2*.

$p21^{WAF-1}$ is a downstream mediator of p53-dependent apoptosis (el-Deiry *et al.* 1994). Recently, Upadhyay *et al.* (1995) reported that *bcl-2* inhibited p53-dependent apoptosis by suppressing the expression of $p21^{WAF-1}$, but did not affect the induction of p53 in response to DNA damage in MCF10A cells. By Western analysis (Figure 11), we found that the level of

$p21^{WAF-1}$ level was high in 184A1 cells, but barely detectable in *bcl-2*-overexpressing clones 4-1 and 4-2. Clone 4-3 showed intermediate levels of both Bcl-2 and $p21^{WAF-1}$. Therefore, in 184A1 cells, $p21^{WAF-1}$ is down-regulated by Bcl-2.

Matrigel assay

The extracellular matrix is important for organization and function of epithelial cells *in vivo*. Matrigel, a solubilized extracellular matrix extracted from Engelbreth-Holm-Swarm mouse sarcoma, consists of extracellular matrix proteins similar to those of the normal mammary basement membrane. Matrigel is often used for *in vitro* studies to mimic *in vivo* conditions. Bergstraesser *et al.* (1993, 1996) reported that normal and tumor-derived HMECs could be distinguished on the basis of their morphology on Matrigel. When plated on Matrigel, primary normal HMECs form three-dimensional structures similar to the ductal and alveolar structures observed in the mammary gland, while malignant cells remain as single and move through Matrigel like tumor cells invading the basement membrane *in vivo*. Immortalized normal human mammary epithelial 184A1 cells also form duct- and alveolus-like structures on Matrigel. As shown in Figure 12, our clones overexpressing *bcl-2* (4-1 and 4-2) did not form structures on Matrigel as efficient by as parental 184A1. Instead many cells remained separate, reminiscent of the behavior of the malignant cells described by Bergstraesser *et al.* (1993,1996). Clone 4-3 showed a phenotype similar to 184A1.

Altogether, these data indicate that overexpression of *bcl-2* may not fully transform HMEC but does confer partially transformed phenotypes, and therefore contributes to mammary tumorigenesis.

Overexpression of bcl-2 in primary HMEC.

Due to the difficulty of transfecting primary HMEC, we looked for more efficient retroviral vectors to transfer genes into primary early-passage HMEC (BE46). We constructed two retroviral vectors, pLNPObcl-2 and pLXSNbcl-2, and introduced into amphotropic packaging cell line, PA317 (Miller *et al.* 1989, 1993). Immunofluorescence staining of PA317 stable transformants indicated that pLNPObcl-2 expressed Bcl-2 protein better than pLXSNbcl-2. Therefore, pLNPObcl-2 retrovirus was used for further studies. HMEC (BE46) at passage 1, grown in DFCI-1 medium, were infected with pLNPObcl-2 retrovirus and selected with 25-50 μg/ml G418. As illustrated in Figure 13, infected cells proliferated well for about two weeks and then became enlarged and vacuolated and eventually senesced the same as the control cells. We therefore conclude that although overexpression of *bcl-2* does provide a survival advantage, it cannot by itself immortalize HMEC.

Immunofluorescence staining showed that Bcl-2 protein was barely detectable in parental BE46 cells, but was highly expressed in more than 90% of retrovirus-infected cells (pLNPObcl-2/BE46). Cytokeratin 19 (K19), an intermediate filament found in differentiated luminal epithelial cells, was highly expressed in most BE46 cells but was expressed at a lower level in fewer than 10% of pLNPObcl-2/BE46 cells. On the other hand, vimentin, an intermediate filament found in fibroblasts, was up-regulated and highly expressed in 50-70% of pLNPObcl-2/BE46 compared to 10-20% of BE46 cells (Table 2). An epithelial-fibroblastoid cell conversion of this kind has been observed in several carcinoma cells both *in vivo* and *in vitro*, and is also found in mammary epithelial cells that are overexpressing oncogenes, such as *c-erbB2*. Lu *et al.* (1995) also observed the epithelial-fibroblastoid cell conversion when *bcl-2* was overexpressed in luminal epithelial cells immortalized by the SV40 large T antigen. We are now testing whether *bcl-2* can cooperate with p53- or Rb-deficiency caused by expression of HPV16 E6 or E7, or with other oncogenes, such as

c-myc, to change phenotypes in primary HMEC; i.e., immotalization, behavior in Matrigel, and expression of differentiation markers.

Conditional Expression System

Comparison of test cells expressing a specific protein with control cells without expression requires a sensitive, reliable and conditional (reversible) gene expression system. Several tetracycline-regulated retroviral vectors have been constructed to allow inducible expression of retroviral inserts after integration of the vector in target cells. Unlike the original two-plasmid system, (Gossen et al.1992, Gossen et al. 1995) the entire system is contained within a single retrovirus. In combination with an amphotropic retroviral packaging system, these vectors will provide conditional gene expression quickly and efficiently in a wide variety of cell types, including primary cultures which are usually hard to transfect.

To determine the biological characteristics of the first of these vectors, LINX (Hoshimaru et al. 1996), we introduced the Green Fluorescent Protein (GFP) into the vector, produced amphotropic retrovirus using the Ampho-Phoenix packaging cell line (obtained from Dr. Nolan, Stanford University) and infected three different breast cancer cell lines with the construct. The results of these experiments, summarized in Table 3, indicate that the LINX vector can be infected into breast cancer cells with efficiencies in excess of 75%. They also indicate that while GFP is a highly stable protein, the overall concentration steadily declines to minimal levels over a period of four to eight days following transcriptional inhibition by the tetracycline derivative, doxycycline (DOX). We are convinced that a conditional expression system will provide the most clear and convincing data. Please note that the results reported in the table below apply to the induction and repression of our GFP marker in mass culture. We anticipate that we will be able to obtain individual clones that show better levels of both expression and repression. We have constructed vectors containing HPV16 E6/E7 gene and BRCA1 anti-sense gene, and are now testing the conditional expression of cloned genes.

Next, we introduced dominant β-catenin genes (N-terminal deletions, dN131 and dN151) into these vectors, produced amphotropic retrovirus using the Ampho-Phoenix packaging cell line and infected primary human mammary epithelial cells. After two weeks of drug selection in either 0.5 μg/ml Puromycin (for pRetro ON and pRetro OFF) or 100 μg/ml G418 (for LINX), cells were treated with or without 10ng/ml doxycycline (DOX) for 48 hours. Total cell extracts were subjected to Western analysis using anti-C-terminal β-catenin antibody (see Figure 17a). To demonstrate that induced dominant β-catenin is functional, cells were infected with LINX vector control and LINX with inducible dominant β-catenin gene (dN131) and subsequently transiently transfected with luciferase reporter construct, TOP FLASH, containing LEF1 responsive element in its promoter (obtained from Dr. Hans Clevers). As shown in Figure 17b the relative activity of the LEF1-reporter construct showed significant increase in promoter activity following induction of β-catenin. Based on these results we have selected the LINX vector for further experimentation. We have now constructed conditional retroviral vectors containing HPV16 E6/E7 genes, dominant negative p53 genes and BRCA1 anti-sense gene. These constructs are currently tested for conditional expressions in HMEC and subsequent phenotypic changes including immortalization and telomerase activation.

Task 2c: does not exist in original SOW.

Task 2d: Identify clones that are expressed differentially between the derivative lines of Task 1 (a and b), and teir parent lines.

Differential Display.

We originally proposed the *Differential Display* method (Liang and Pardee 1992) to identify genes that are modulated by p53 and BRCA1 deficiency. As our initial experimental model we selected to compare purified normal colonic crypt cells to crypt cells isolated from adenomatous colonic polyps. While the biologic function of breast and colonic epithelial cells differ from each other, the rationale for using colonic crypt cells is firstly based on the fact that the human colonic adenomas are deficient in the APC tumor suppressor protein, which has been shown in mouse to be predisposing for mammary carcinoma as well as colon carcinoma (Moser et al. 1995; Moser et al. 1993). Furthermore, many human mammary tumors have been shown to be deficient in E-cadherin (Kanai et al. 1994; Rimm et al. 1995; Schmutzler et al. 1996), an important cell adhesion protein whose activity is modulated by APC and beta-catenin, each of which are members of the Wnt regulatory pathway (Tao et al. 1996; Vleminckx et al. 1997). It is also worth noting that Wnt-1 is a gene first identified as the target gene for mouse mammary tumor virus in MMTV-induced mouse mammary tumors. As our experimental procedure, we prepared first strand cDNA from total RNA isolated from either normal or adenomatous crypt cells using a collection of twelve anchored poly(T) down-stream primers. Each of the first strand cDNAs thus synthesized subsequently served as template in a PCR reaction against twenty different arbitrarily designed up-stream primers. A total of 240 sample-pairs were prepared in this way and the resulting radiolabeled PCR products visualized in acrylamide gels. To confirm reproducibility of the PCR band patterns all samples were prepared and tested in duplicate (Figure18). Our Differential Display comparison of the normal and adenomatous colonic crypt cells has been completed, resulting in the identification of at least three genes (CGM2, prothymosin α, and a novel gene with similarity to X box binding protein-1) which consistently and reproducibly show altered expression levels in a panel of two normal and six polyps (Figure 19) (manuscript submitted). In addition to these three genes more than 30 genes reproducibly displayed altered expression levels in the Differential Display gels, however the very low abundance of these messages in the tissue samples we analyzed prevented us from confirming their exact expression status in traditional methods like Northern Blot analysis and RNase Protection Assay.

Microarray Expression Profiles.

Several new hybridization-based methodologies to quantitatively measure expression levels of large numbers of arrayed genes have been described during the past several years (Fodor et al. 1993; Pease et al. 1994; Schena et al. 1995, DeRisi et al. 1996). While the concept and biochemical principles of this type of analysis are simple, the implementation requires sophisticated and costly robotics and laser-scanning technology that is not readily available. Therefore, to gain access to this technology, our laboratory has established a collaboration with Molecular Dynamics/Amersham, which has developed a full set of instrumentation for creating and reading cDNA microarrays.

The microarray assay is based on a collection of cDNA clones arrayed onto a glass slide. This array is subsequently tested by hybridization against fluorescently-labeled first-strand cDNA generated from tissue mRNA. The strength of the fluorescent signal measured for each of the cDNA clones present on the array correlates to the abundance of that specific mRNA in the tissue. The Molecular Dynamics Microarray Scanner permits the simultaneous detection of two differently-labeled fluorescent probes. The ability to distinguish between two independent fluorescent signals in a single assay allows for direct comparison of gene expression patterns between two tissues in a single experiment. This feature is particularly useful for experiments where

a cell population harboring a conditional expression vector is compared with respect to induced versus suppressed conditions.

The DNA used as the hybridization target on the slides is prepared from selected cDNA clones. We have now obtained a collection of more than 23,000 minimally redundant cDNA clones, which are arranged in a 96-well microtitre dish format, permitting efficient plasmid purification, PCR amplification and PCR product purification. In our current protocol, a 150μl bacterial culture is grown and lysed using alkaline lysis procedures in a standard round-bottom microtitre dish. Following centrifugation, the plasmid DNA solution is transferred to a Millipore MAHV N45 filter-bottom microtitre dish with 150μl of DNA Purification Resin (Promega). Plasmid DNA eluted from this mini-column method is of high purity and provides an excellent template for PCR amplification of the insert. A second 96-well mini-column purification step separates PCR products from unincorporated nucleotides and primers to ensure that the target DNA performs optimally on the array slide. Prior to deposition on the microarray spotter, target DNA is mixed with a proprietary agent from Amersham. DNA is then bonded to glass slides by UV-cross linking. The microarray spotter is designed to accept the 96-well format and will host eight individual plates per loading. In its current configuration, the spotter can array over 4500 unique DNA targets in duplicate on a single microscope slide.

To measure the expression profile (i.e., the relative abundance of individual mRNA species) from a specific cell culture, we will first extract total RNA from the cells using the TriZol reagent. mRNA is isolated from total RNA samples using Qiagen's Oligotex mRNA isolation procedure, then transcribed into first-strand cDNA using AMV reverse transcriptase, following the protocol provided by Amersham. During this process, DNA is labeled by incorporating Cy3 or Cy5 fluorescently-tagged nucleotides at a rate of approximately 1 tag per 100 nucleotides). To minimize any possible bias of the relative abundance of the individual species of mRNA, labeled first-strand cDNA is not further amplified following synthesis. Hybridization takes place under a sealed cover slip in a low buffer volume to achieve the highest possible probe concentration. Once slides are washed and scanned, the expression profile can be established and analysed using ImageQuaNT software, a dedicated computer-based image analysis program developed by Molecular Dynamics.

Analysis of primary breast cells with conditionally induced dominant β-catenin.

β-catenin has resently been shown to act as an oncogene in certain biologic models and to study the gene regulatory effects of the cancer pathway driven by wnt-1, APC or β-catenin in breast cells. Human primary epithelial mammary cells were infected with a conditionally suppressible dominant β-catenin retroviral construct as mentioned above. Excessive stimulation of this pathway and certain types of mutations have been shown to involve the formation of a persistent transcriptionally active complex of β-catenin and LEF1. mRNA from several different primary breast cultures, with and without induced β-catenin, was prepared and fluorescently labeled for dual color hybridization on microarray slides representative of 2400 unique cDNAs. A total of twenty-nine different genes have been identified as differentially expressed and are listed in Table 4. To confirm that the microarray observations are correct, Northern analysis of each differentially expressed gene is being undertaken. In figure 4 we show that Psoriasin, which displayed a 3-4 fold increase in abundance judging from the microarray analysis reveal similar differences in abundance when tested by Northern analysis.

Analysis of primary breast cells deficient in p53/Rb functions.

The E6 and E7 genes derived from human papilloma virus-type 16 have been shown to bind to the tumor suppressor genes Rb and p53, and our studies have shown that these genes can immortalize different populations of primary epithelial breast cells (submitted). We have established several primary epithelial mammary cell cultures with either E6 alone, E7 alone, or E6 and E7 together. As part of our experiment design we compared gene expression profiles in these lines against one another on microarray slides representative of 2400 unique cDNAs. The genes listed in Table 5 showed 3× fold or more variation in expression levels in a comparison between human mammary epithelial cells, with E6 (green) and with E6/E7 (red).

Task 2e: Characterize differentially expressed genes on breast-tumor cells and tissue samples.

During the pat 12 months, most of our efforts have been focused on the completion of Task 2d in our statement of work. It has been our primary goal to establish microarray analysis as a reliable and reproducible technology to compare gene expression profiles and identify differentially regulated genes. Now experiments have been carried out to scan gene expression profiles (red/green signal) between parental HMEC and HMEC stably transduced with E6, E7, E6E7, or dominant negative p53, within our collection of more than 23,000 minimally redundant cDNA clones. Work has been in progress to analyze enormous amount of numerical data to obtain the specific gene expression patterns among different cell types.

Meanwhile, during the process of establishing the fine detection method for BRCA1 protein, we have discovered that BRCA1 protein is associated with centrosomes during mitosis, on the basis of immunofluorescence staining of whole cells and biochemical analysis of isolated centrosomes. We also show that BRCA1 interacts with γ-tubulin, a key structural component of the centrosome. We suggest that BRCA1 may interact with other centrosome components to help control appropriate assembly of mitotic spindles and regulate G2/M progression, or to modify the BRCA1 protein itself to prepare for the next cell cycle. BRCA1 protein might also associate with the centrosomes in order to ensure appropriate distribution to the two daughter cells.

BRCA1 encodes a protein of 1863 amino acids (~220-kDa). The presence of an NH_2-terminal zinc-ring domain and a COOH-terminal transactivation domain suggest that BRCA1 might be a transcription factor (Miki 1994). Indeed, BRCA1 contains two putative nuclear localization signals (Chen 1995), and its COOH-terminal domain shows transcription-activation activity when fused to the GAL4 DNA-binding domain (Chapman 1996, Monteiro 1996). BRCA1 protein is a component of the RNA polymerase complex (Scully 1997), and co-activates p53-mediated transcription (Ouchi 1998). As BRCA1 also forms a complex with rad51 in mitotic and meiotic chromosomes, it may be involved in DNA repair and the maintenance of genomic integrity (Scully 1997). Knockout experiments in mice have revealed that BRCA1 might be required for cell proliferation, because homozygous *BRCA1* knockout mice die at an early stage of embryogenesis (Gowen 1996, Hakem 1996).

BRCA1 protein is mainly localized in the nucleus (Scully 1996). It is expressed and phosphorylated in a cell cycle-dependent fashion (Chen 1996, Ruffner 1997); the mRNA increases at G1/S, remains high through S and G2/M, and decreases in G1. Some investigators have reported that protein and mRNA levels rise and fall in parallel during progression of the cell cycle (Vaughn 1996, Gudas 1996), but others have seen no obvious changes in protein concentration (Aprelikova 1996). BRCA1 is phosphorylated in S and M phases (Chen 1996, Ruffner 1997, Thomas 1997) and

after DNA damage (Thomas 1997, Scully 1997). However, when MCF-7 cells are arrested in G2/M by colchicine, most of their BRCA1 protein is hypophosphorylated (Thomas 1997).

The centrosome controls assembly of microtubules, a process that plays a central role in organizing cell structure, determining cell polarity, directing cell movement during interphase, and orchestrating formation of the bipolar spindle during mitosis (Kellogg 1994). In mammalian cells the centrosome is comprised of a pair of centrioles (short cylinders constructed from nine triplet microtubules consisting of α/β tubulin dimers) and amorphous pericentriolar material. The centrosome normally duplicates once during each cell cycle starting at the G1/S transition; duplication is usually completed by G2. As mitosis begins, the two centrosomes separate to organize the bipolar mitotic spindle. The centrosome contains hundreds of proteins, some of which have been identified, e.g. γ-tubulin (Zheng 1991, Stearns 1991) and pericentrin (Doxsey 1994). Both are components of pericentriolar material. γ-Tubulin is associated with the minus-end of microtubules and is responsible for their nucleation (Stearns 1994).

An increasing number of proteins that regulate the cell cycle, especially those that control G2/M progression, have been localized to the centrosome; cyclin A, cyclin B (Bailly 1989), $p34^{cdc2}$ (Bailly 1989, Pockwinse 1997), and 14-3-3 (Pietromonaco 1996) are examples. Brown *et al.* reported that the p53 tumor suppressor is also associated with the centrosome in interphase cells (1994); moreover, p53-/- mouse embryonic fibroblasts show a high frequency of abnormal mitoses with amplified centrosomes (Fukasawa 1996). pRB is also present in mitotic spindles and centrosomes during mitosis (Thomas 1996), but deficiency of pRB does not affect centrosome duplication (Fukasawa 1996).

BRCA1 is Localized to the Centrosome during Mitosis.

Two BRCA1-specific antibodies were used for these studies: MS110, a mouse monoclonal antibody raised against a BRCA1-GST fusion protein containing amino acids 1 to 304 of human BRCA1 protein (Scully 1996), and C-20, a rabbit polyclonal antibody raised against a peptide corresponding to amino acids 1843-1862 of human BRCA1. Immunofluorescence staining of a population of replicating COS-7 cells revealed the usual dot pattern in the nucleus. However, a unique staining pattern reminiscent of centrosomes was observed in mitotic cells (Fig. 20, 21).

To confirm the localization of BRCA1 protein at mitotic centrosomes, we conducted a series of double-staining experiments using C-20 and MS110 for BRCA1 staining, γ-tubulin and pericentrin antibodies for centrosome staining, and α-tubulin antibody for microtubule staining. In addition, DAPI staining of DNA was used to locate the nucleus. Double-staining of COS-7 cells with γ-tubulin antibody and BRCA1 C-20 antibody provided direct evidence for the presence of BRCA1 protein at mitotic centrosomes. Two-color (BRCA1+γ-tubulin) or three-color (BRCA1+γ-tubulin+ DAPI) composite images showed colocalization of the BRCA1 and γ-tubulin signals at mitotic centrosomes (Fig. 20). The concentration of BRCA1 signal at mitotic centrosomes was apparent from prometaphase to metaphase (Fig. 20*A*) and early anaphase (Fig. 20*B*). As with γ-tubulin (Fig. 20) (Stearns 1991), BRCA1 staining diminished at the centrosome as cells proceeded to late anaphase (Fig. 20*C*) and telophase (data not shown). Results were similar when COS-7 cells were co-stained with MS110 (Fig. 2*a*) and pericentrin antibody (Fig. 21*b*). Both BRCA1 MS110 (Fig. 21*d*) and C-20 (Fig. 21*e*) stained mitotic centrosomes. In contrast, interphase cells had one or two centrosomes juxtaposed to the nucleus (Fig. 21*g*) and exhibited only nuclear dot staining pattern of BRCA1 (Fig. 21*h*), with no overlap between the nuclear BRCA1 dots and the interphase

centrosomes (Fig. 21*g-i*). The same staining results were obtained whether the fixative was neutral paraformaldehyde or methanol. Control experiments using normal mouse IgG and rabbit IgG to replace primary antibodies or using C-20 peptide to block C-20 antibody did not show staining of the centrosome (data not shown).

BRCA1 was also present at mitotic centrosomes of breast epithelial cells (BE46, E6/BE46, and 184A1), adenovirus-transformed human kidney 293 cells, and breast cancer MCF7 cells. An example of E6/BE46 co-stained with α-tubulin antibody and BRCA1 C-20 is seen in Fig. 21*j-l* and shows the BRCA1 signal concentrated at the spindle poles.

220-kDa BRCA1 Protein is Present in Isolated Centrosomes.

Centrosomes were isolated from COS-7 and MCF7 cells by discontinuous sucrose gradient fractionation (Moudjou 1994) and subjected to SDS-PAGE and Western analysis. The cells were harvested for these procedures after brief treatment with nocodazole and cytochalasin D to disrupt microtubules and the actin cytoskeleton. Fractions enriched for centrosomes were indicated by the presence of γ-tubulin.

BRCA1 protein was detected by Western hybridization with the MS110 antibody. As shown in Fig. 22*A*, the distribution of 220-kDa BRCA1 protein among the fractions parallels the distribution of γ-tubulin; the BRCA1 and γ-tubulin protein signals were strongest in fractions 2 and 3, corresponding to 55~60% w/w sucrose. Due to variation of the sucrose gradient, the strongest signal sometimes concentrated only in one fraction as in Fig. 22*B* control. However, only a small portion of the total BRCA1 protein was present in the centrosome fractions. To eliminate the possibility of contamination with interphase nuclei that have abundant BRCA1 protein, the same blot was probed with lamin antibodies. We detected no lamins in the centrosome fractions (Fig. 22*A*). Results were the same with MCF7 cells (data not shown). These biochemical data confirmed the presence of 220-kDa BRCA1 protein at the centrosome.

BRCA1 Protein is Enriched in Centrosomes Isolated from Cells Arrested in G2/M.

Levels of BRCA1 protein in centrosome fractions from exponentially growing COS-7 cells were compared with their counterparts from cells arrested in G2/M. Cells were incubated with 2 μM thymidine for 10-12 hours and then with 1 μM nocodazole for 12-14 hours at 37°C (Krek 1995). Flow cytometric analysis indicated that the G2/M population was enriched 3- to 4-fold by this treatment (Fig. 22*B*). Centrosome preparations from equal numbers of control and mitosis-arrested cells were subjected to Western analysis. Two components of the mitotic cyclin-dependent kinase, cyclin B and $p34^{cdc2}$, were used as controls; both of these proteins accumulate at the centrosome in a cell cycle-dependent manner (Bailly 1989, 1992). γ-Tubulin served as the indicator for centrosome fractions. Cyclin B, $p34^{cdc2}$, γ-tubulin, and BRCA1 were each enriched in the centrosome fractions from COS-7 cells arrested in G2/M; the level of BRCA1 protein in these centrosomes was 3-4 times the amount seen in control cells (Fig 22*B*). No lamin was detected in the centrosome fractions.

Association Between γ-tubulin and BRCA1.

The association between BRCA1 and the mitotic centrosome was further confirmed by co-immunoprecipitation of BRCA1 and γ-tubulin protein. Western blot analysis demonstrated that both were present in the immunoprecipitate generated from COS-7 cells by BRCA1 C-20 antibody. MS110 was used to detect the BRCA1 and γ-tubulin antibody for γ-tubulin (Fig. 23, lane 2). α-Tubulin was not immunoprecipitated by C-20 (data not shown). No BRCA1 or γ-tubulin proteins were detected using rabbit IgG, the negative control (Fig. 23, lane 1). When C-20 peptide was

added to block the C-20 antibody, neither BRCA1 nor γ-tubulin was immunoprecipitated (data not shown). Reciprocally, monoclonal γ-tubulin antibody, but not mouse IgG, also brought down BRCA1 protein (Fig. 23, lanes 3 and 4). These results indicate that a specific, but perhaps not direct, interaction between γ-tubulin and BRCA1 does occur.

The phosphorylation status of BRCA1 varies during the cell cycle. This phosphoprotein migrates as a ~220-kDa doublet upon 6% SDS-PAGE (Scully 1996). The more slowly migrating band that corresponds to the hyperphosphorylated isoform of BRCA1 is predominant in S phase (Chen 1996, Ruffner 1997, Thomas 1997). A more rapidly migrating band represents the hypophosphorylated isoform (Scully 1996, 1997). In our experiments, BRCA1 immunoprecipitated by γ-tubulin antibody appears to migrate slightly faster than BRCA1 immunoprecipitated by C-20 from whole cell lysates (Fig. 23). To test whether BRCA1 is hypophosphorylated when associated with γ-tubulin, we resolved immunoprecipitated samples on a 4-12% SDS polyacrylamide gel with longer separation times to better resolve high-molecular-weight proteins. As shown in Fig. 24, the BRCA1 protein immunoprecipitated by γ-tubulin antibody (lane 4), or present in isolated centrosomes (lane 1), corresponded to the hypophosphorylated form, which co-migrates with *in vitro*-translated BRCA1 (lanes 2 and 3). The majority of BRCA1 protein immunoprecipitated by C-20 migrated more slowly (Fig. 24, lane 5), however, the hypophosphorylated BRCA1 band was visible after longer exposure (data not shown). To exclude the possibility that the BRCA1 associated with the centrosome might not be a full-length protein, the blot containing lanes 1-2 was hybridized with D-20, a rabbit polyclonal antibody raised against amino acids 2-21 of human BRCA1 protein; with MS13, which recognizes the N-terminal region of BRCA1; and with C-20, which recognizes the C-terminal region of BRCA1. All these antibodies recognized the BRCA1 protein in the isolated centrosomes (data not shown), indicating that the hypophosphorylated BRCA1 associated with the centrosome is a full-length protein.

In summary, we provide here the first evidence demonstrating an association of BRCA1 protein with the centrosome in mitotic cells. This evidence includes the results of immunofluorescence microscopy using polyclonal and monoclonal BRCA1-specific antibodies that recognize a C-terminal and an N-terminal domain of the protein respectively (Fig. 20, 21). Biochemical analysis of isolated centrosomes further supports the presence of 220-kDa BRCA1 protein in the centrosomes (Fig. 22*A*). Furthermore, quantitative analysis of the 220-kDa BRCA1 protein associated with centrosomes isolated from equal numbers of exponentially growing control cells and cells arrested in G2/M (Fig. 22*B*) indicates that the enrichment of BRCA1 in arrested cells is proportional to the enrichment of the G2/M population. This observation is consistent with results of immunofluorescence staining that localize BRCA1 to centrosomes in mitotic cells but not in interphase cells.

Co-immunoprecipitation of BRCA1 with γ-tubulin (Fig. 23) suggests an interaction between these two proteins. γ-Tubulin, a crucial component of the centrosome, is responsible for nucleation of microtubules. It forms complexes with other components of the centrosome such as pericentrin (Dictenberg 1998), and mammalian homologues of the yeast spindle pole body components Spc97p and Spc98p (Murphy 1998, Tassin 1998). However, to our knowledge, BRCA1 is the first tumor suppressor protein found to be associated with γ-tubulin, albeit perhaps indirectly, an observation that suggests that BRCA1 may be a regulator of mitotic-spindle assembly and of the G2/M checkpoint. Supporting evidence for involvement of BRCA1 in regulation of G2/M comes from a

discovery by Larson *et al.* that over-expression of a dominant-negative COOH-terminal peptide containing amino acids 1293-1863 alters G2/M progression and results in a decrease of the G2/M population and a reduction in the efficacy of colchicine in inducing G2/M arrest (Larson 1997). It is also possible that BRCA1 associates with centrosomes during mitosis as a way to achieve appropriate distribution between the two daughter cells, as may be the case with other nuclear proteins such as NuMA (Compton 1992), a molecule that also is required for the proper completion of mitosis (Compton 1993). We also show that the BRCA1 protein associated with the centrosomes is hypophosphorylated (Fig. 24), suggesting that phosphorylation status may be important in determining the centrosome functions and/or subcellular distribution of BRCA1, or may be the result of its association with the centrosome.

BRCA1 is involved in progression of the cell cycle. Its expression and phosphorylation are cell cycle-dependent, and over-expression induces growth arrest (Somasundaram 1997) or apoptosis (Shao 1996). On the other hand, cellular proliferation is accelerated when BRCA1 expression is suppressed by antisense oligonucleotides (Thompson 1995) or by over-expression of dominant-negative BRCA1 peptides (Larson 1997). Furthermore, breast tumors carrying BRCA1 mutations accumulate more chromosomal abnormalities (Tirkkonen 1997) compared to breast tumors without BRCA1 mutations. It is likely that BRCA1 plays a continuous role throughout the cell cycle: expression and phosphorylation is induced at G1/S transition, and a complex with rad51 is associated with chromosomes during S phase and participates in DNA repair (Scully 1997). Moreover, as a component of RNA polymerase II (Scully 1997) or as a coactivator of p53-mediated transcription (Ouchi 1998), BRCA1 may regulate the expression of other genes required for cell cycle progression. An increasing number of proteins involved in the G2/M checkpoint are found to associate with centrosomes during cell cycling, e.g. cyclin B (Bailly 1992), $p34^{cdc2}$ (Bailly 1989, Pockwinse 1997), p53 (Brown 1994), and 14-3-3 (Pietromonaco 1996). Therefore, it is possible that BRCA1 also plays a functional role with mitotic centrosomes.

(7) CONCLUSIONS

During the funded years, we had produced good progress in establishing and characterizing HMEC deficient in p53 gene functions, although there were some setbacks due to unexpected technical difficulties. Early- and late-passage HMEC carrying HPV16 E6 and/or E7 genes have been characterized for some key properties acquired during malignant transformation, including immortalization, telomerase acivation, and insensitivity to growth inhibibition by TGF-β. One drawback is that E6 and E7 proteins bind not only p53 and Rb, respectively, but also bind other cellular proteins, complicating the data analysis. Our recent establishment of immortalized HMEC by dominant negative p53 genes would answer this concern. On the other hand, construction of HMEC deficient in BRCA1 gene functions still remain to be performed because time has not yet allowed us to create such cells in an effective manner.

Although it was not included in our original SOW, our recent discovery that BRCA1 protein is associated with mitotic centrosome suggests totally new role of BRCA1 for cell cycle progression.

In addition, our recent acquisition of the Microarray Spotting and Scanning techniques and over 23,000 minimally redundant cDNA target samples will help us to analyze expression profiles from distinct breast cell lines we have created. We firmly believe that this system will provide us critical information to our understanding of breast carcinogenesis.

(8) REFERENCES

Adams, P.D. and Kaelin, W.G. Jr. (1996) *Curr. Top. Microbiol. Immunol.* **208,** 79-93

Aprelikova, O., Kuthiala, A., Bessho, M., Ethier, S., & Liu, E.T. (1996) *Oncogene* **13**, 2487-2491.

Bailly, E., Pines, J., Hunter, T., & Bornens, M (1992) *J. Cell Sci.* **101**, 529-545.

Bailly, E., Doree, M, Nurse, P., & Bornens, M (1989) *EMBO J.* **8**, 3985-3995.

Band, V. and Sager, R. (1989) *Proc. Natl Acad. Sci. U S A* **86,** 1249-1253

Band, V., De Caprio, J.A., Delmolino, L., Kulesa, V. and Sager, R. (1991) *J. Virol.* **65,** 6671-6676

Barth AI, Pollack AL, Altschuler Y, Mostov KE, Nelson WJ. J Cell Biol 136:693-706 (1997).

Bodnar AG, Ouellette M, Frolkis M, Holt SE, Chiu CP, Morin GB, Harley CB, Shay JW, Lichtsteiner S, Wright WE *Science* (1998) 279: 349-52

Brown, C.R., Doxsey, S.J., White, E., & Welch, W.J. (1994) *J. Cell. Physiol.* **160**, 47-60.

Bryan, T.M., Englezou, A., Gupta, J., Bacchetti, S., and Reddel, R.R. (1995) *EMBO J.* 14, 4240-4248

Cao, Y., Gao, Q., Wazer, D.E., & Band, V. (1997) *Cancer Research* **57,** 5584-5589.

Chapman, M.S., & Verma, I.M. (1996) *Nature* **382**, 678-679.

Chen, Y., Chen, C.-F., Riley, D.J., Allred, D.C., Chen, P.-L., Von Hoff, D., Osborne, C.K., & Lee, W.-H. (1995) *Science* **270**, 789-791.

Chen, Y., Farmer, A.A., Chen, C.-F., Jones, D.C., Chen, P.-L., & Lee, W.-H. (1996) *Cancer Res.* **56**, 3168-3172.

Compton, D.A., Szilak, I., & Cleveland, D.W. (1992) *J. Cell Biol.* **116**, 1395-1408.

Compton, D.A., & Cleveland, D.W. (1993) *J. Cell Biol.* **120**, 947-957.

Couch, F.J., Weber, B.L., & the Breast Cancer Information Core (1996) *Hum. Mutat.* **8**, 8-18.

DeRisi J, Penland L, Brown PO, Bittner ML, Meltzer PS, Ray M, Chen Y, Su YA, Trent JM. Nat Genet 14:457-460 (1996).

Dictenberg, J.B., Zimmerman, W., Sparks, C.A., Young, A., Vidair, C., Zheng, Y., Carrington, W., Fay, F.S., & Doxsey, S.J. (1998) *J. Cell Biol.* **141**, 163-174.

Doxsey, S.J., Stein, P., Evans, L., Calarco, P.D., & Kirschner, M. (1994) *Cell* **76**, 639-650.

Fodor S, Rava R, Huang X, Pease A, Holmes C, Adams C. Nature 364:555-556 (1993).

Foster SA, Galloway DA *Oncogene* 1996 Apr 18;12(8):1773-9

Foster SA, Wong DJ, Barrett MT, Galloway DA *Mol Cell Biol* 1998 Apr;18(4):1793-801

Fukasawa, K., Choi, T., Kuriyama, R, Rulong, S, & Vande Woude, G.F. (1996) *Science* **271**, 1744-1747.

Gossen M, Bujard H. Proc Natl Acad Sci U S A 89:5547-5551 (1992).

Gossen M, Freundlieb S, Bender G, Muller G, Hillen W, Bujard H. Science 268:1766-1769 (1995).

Gowen, L.C., Johnson, B.L., Latour, A.M., Sulik, K.K., & Koller, B.H. (1996) *Nat. Genet.* **12**, 191-194.

Greider, C.W. (1998) *Proc. Natl. Acad. Sci. U S A* **95,** 90-92

Gudas, J.M., Li, T., Nguyen, H., Jensen, D., Rauscher, F.J. III, & Cowan, K.H. (1996) *Cell Growth & Differ.* **7**, 717-723.

Hakem, R., de la Pompa, J.L., Sirard, C., Mo, R., Woo, M.,*et al.* (1996) *Cell* **85**, 1009-1023.

Halbert CL, Demers GW, Galloway DA. J Virol 65:473-478 (1991).

Hammond, S.L., Ham, R.G. & Stampfer, M.R. (1984) *Proc. Natl Acad. Sci. U S A* **81,** 5435-5439

Hawley-Nelson, P., Vousden, K.H., Hubbert, N.L., Lowy, D.R. and Schiller, J.T. (1989) *EMBO J.* **8,** 3905-3910

Hofmann A, Nolan GP, Blau HM. Proc Natl Acad Sci U S A 93:5185-5190 (1996).

Hoshimaru M, Ray J, Sah D, Gage F. Proc Natl Acad Sci U S A 93:1518-1523 (1996).

Jiang XR, Jimenez G, Chang E, Frolkis M, Kusler B, Sage M, Beeche M, Bodnar AG, Wahl GM, Tlsty TD, Chiu CP *Nat Genet* 1999 Jan;21(1):111-4

Kaelin, W.G. Jr. *et al.* (1992) *Cell* **70,** 351-364

Kern, S.E. *Gastroenterology* (1994) **106,** 1708-1711.

Kellogg, D.R., Moritz, M., & Alberts, B.M. (1994) *Annu. Rev. Biochem.* **63**, 639-674.

Kim, N.W., Piatyszek, M.A., Prowse, K.R., Harley, C.B., West, M.D., Ho, P.L., Coviello, G.M., Wright, W.E., Weinrich, S.L. and Shay, J.W. (1994) *Science* **266,** 2011-2015

Kiyono T, Foster SA, Koop JI, McDougall JK, Galloway DA, Klingelhutz AJ *Nature* (1998) 396: 84-8

Klingelhutz, A.J., Foster, S.A. and McDougall, J.K. (1996) *Nature* 380, 79-82

Krek, W., & DeCaprio, J.A. (1995) *Methods. Enzymol.* **254**, 114-124.

Larson, J.S., Tonkinson, J.L., & Lai, M.T. (1997) *Cancer Res.* **57**, 3351-3355.

Li, M.L., Aggeler, J., Farson, D.A., Hatier, C., Hassell, J., and Bissell, M.J. 1987. *Proc. Natl. Acad. Sci.* 84: 136-140.

Liang P, Pardee A. Science 257:967-971 (1992).

Miki, Y., Swensen, J., Shattuck-Eidens, D., Futreal, P.A., Harshman, K., *et al.* (1994) *Science* **266**, 66-71.

Miller, A.D., Miller, D.G., Garcia, J.V. and Lynch, C.M. (1993) *Methods Enzymol.* 217, 581-599

Monteiro, A.N.A., August, A., & Hanafusa, H. (1996) *Proc. Natl. Acad. Sci. USA* **93**, 13595-13599.

Morales CP, Holt SE, Ouellette M, Kaur KJ, Yan Y, Wilson KS, White MA, Wright WE, Shay JW. *Nat Genet* 1999 Jan 21:1 115-8

Moudjou, M., & Bornens, M. (1994) in *Cell Biology: A Laboratory Handbook*, ed. Celis, J.E. (Academic Press, San Diego.), pp. 595-604.

Murphy, S.M., Urbani, L., & Stearns, T. (1998) *J. Cell Biol.* **141**, 663-674.

Newman, B., Mu, H., Butler, L.M., Millikan, R.C., Moorman, P.G., & King, M.-C. (1998) *JAMA* **279**, 915-921.

Ouchi, T., Monteiro, A.N.A., August, A., Aaronson, S.A., & Hanafusa, H. (1998) *Proc. Natl. Acad. Sci. USA* **95**, 2302-2306.

Paulus W, Baur I, Boyce FM, Breakefield XO, Reeves SA. J Virol 70:62-67 (1996).

Pear, W.S., Nolan, G.P., Scott, M.L. and Baltimore, D. (1993) *Proc. Natl Acad. Sci. U S A* **90,** 8392-8396

Pease A, Solas D, Sullivan E, Cronin M, Holmes C, Fodor S. Proc Natl Acad Sci U S A 91:5022-5026 (1994).

Petersen, O.W., & van Deurs, B. (1987) *Cancer Res.* **47**, 856-866.

Petersen, O.W., Ronnov-Jessen, L., Howlett, A.R., and Bissell, M.J. 1992. *Proc. Natl. Acad. Sci.* 89: 9064-9068.

Pietromonaco, S.F., Seluja, G.A., Aitken, A., & Elias, L. (1996) *Blood Cells Mol. & Dis.* **22**, 225-237.

Pockwinse, S.M., Krockmalnic, G., Doxsey, S.J., Nickerson, J., Lian, J.B., van Wijnen, A.J., Stein, J.L., Stein, G.S., & Penman, S. (1997) *Proc. Natl. Acad. Sci. USA* **94**, 3022-3027.

Pollack AL, Barth AIM, Altschuler Y, Nelson WJ, Mostov KE. J Cell Biol 137:1651-1662 (1997).

Reznikoff, C.A. *et al.* (1994) *Genes Dev.* **8,** 2227-2240

Ruffner, H., & Verma, I.M. (1997) *Proc. Natl. Acad. Sci. USA* **94**, 7138-7143.

Schena M, Shalon D, Davis RW, Brown PO. Science 270:467-470 (1995).

Scully, R., Anderson, S.F., Chao, D.M., Wei, W., Ye, L., Young, R.A., Livingston, D.M., & Parvin, J.D. (1997) *Proc. Natl. Acad. Sci. USA* **94**, 5605-5610.

Scully, R., Chen, J., Plug, A., Xiao, Y., Weaver, D., Feunteun, J., Ashley, T., & Livingston, D.M. (1997) *Cell* **88**, 265-275.

Scully, R., Ganesan, S., Brown, M., De Caprio, J.A., Cannistra, S.A., Feunteun, J., Schnitt, S., Livingston, D.M. (1996) *Science* **272**, 123-125.

Scully, R., Chen, J., Ochs, R.L., Keegan, K., Hoekstra, M., Feunteun, J., & Livingston, D.M. (1997) *Cell* **90**, 425-435.

Shao, N., Chai, Y.L., Shyam, E., Reddy, P., & Rao, V.N. (1996) *Oncogene* **13**, 1-7.

Shay JW, Wright WE, Brasiskyte D, Van der Haegen BA *Oncogene* 1993 Jun;8(6):1407-13

Shay, J.W., Wright, W.E., Brasiskyte, D. and Van der Haegen, B.A. (1993) *Oncogene* **8,** 1407-1413

Somasundaram, K., Zhang, H., Zeng, Y.-X., Houvras, Y., Peng, Y., Zhang, H., Wu, G.S., Licht, J.D., Weber, B.L., & El-Deiry, W.S. (1997) *Nature* **389**, 187-190.

Stampfer, M., Hallowes, R.C. and Hackett, A.J. (1980) *In Vitro* **16,** 415-425

Stampfer, M.R., & Bartley, J.C. (1985) *Proc. Natl. Acad. Sci. USA* **82**, 2394-2398.

Stearns, T., Evans, L., & Kirschner, M. (1991) *Cell* **65**, 825-836.

Stearns, T. & Kirschner, M. (1994) *Cell* **76**, 623-637.

Stöppler, H., Hartman, D.-P., Sherman, L. and Schlegel, R. (1997) *J. Biol. Chem.* **272,** 13332-13337

Szabo, C.I., & King, M.-C. (1995) *Hum. Mol. Genet.* **4**, 1811-1817.

Tassin, A.-M., Celati, C., Moudjou, M, & Bornens, M. (1998) *J. Cell Biol.* **141**, 689-701.

Thomas, J.E., Smith, M., Tonkinson, J.L., Rubinfeld, B., & Polakis, P (1997) *Cell Growth & Differ.* **8**, 801-809.

Thomas, R.C., Edwards, M.J., & Marks, R. (1996) *Exp. Cell Res.* **223**, 227-232.

Thompson, M.E., Jensen, R.A., Obermiller, P.S., Page, D.L., & Holt, J.T. (1995) *Nat. Genet.* **9**, 444-450.

Tirkkonen, M., Johannsson, O., Agnarsson, B.A., Olsson, H., Ingvarsson, S., Karhu, R., Tanner, M., Isola, J., Barkardottir, R.B., Borg, A., & Kallioniemi, O.-P. (1997) *Cancer Res.* **57**, 1222-1227.

Vaughn, J.P., Davis, P.L., Jarboe, M.D., Huper, G., Evans, A.C., Wiseman, R.W., Berchuck, A., Iglehart, J.D., Futreal, P.A., & Marks, J.R. (1996) *Cell Growth & Differ.* **7**, 711-715.

Wazer, D.E., Liu, X.L., Chu, Q., Gao, Q. and Band, V. (1995) *Proc. Natl Acad. Sci. U S A* **92,** 3687-3691

Weaver V, Fischer A, Peterson O, Bissell M. Biochem Cell Biol 74:833-51 (1996).

Weaver V, Petersen O, Wang F, Larabell C, Briand P, Damsky C, Bissell M. J Cell Biol 137:231-45 (1997).

Wang, J.Y. (1997) *Curr. Opin. Genet. Dev.* 7, 39-45

Wang J, Xie LY, Allan S, Beach D, Hannon GJ (1998) *Genes Dev* 12:1769-74

Weinberg, R.A. (1996) *Cell* **85,** 457-459

Wright, W.E., Shay, J.W. and Piatyszek, M.A. (1995) *Nucleic Acids Res.* **23,** 3794-3795

Yu JS, Sena-Esteves M, Paulus W, Breakefield XO, Reeves SA. Cancer Res 56:5423-5427 (1996).

Zheng, Y., Jung, M.K., & Oakley, B.R. (1991) *Cell* **65**, 817-823.

Appendices

MATERIALS AND METHODS

Isolation and culture of primary HMEC- Breast organoids consisting of ductal and lobuloalveolar fragments, were prepared from reduction mammoplasty tissue specimens and frozen by the methods of Stampfer et al. (1980). To culture HMEC, thawed organoids were washed in cold Dulbecco's phosphate-buffered saline and then digested with trypsin-EDTA (0.05% / 0.02 % in PBS) for 20 min at 37°C. Cells were washed three times, counted, and cultured in the mixture (50% / 50%) of fresh and conditioned DFCI-1 medium (Wazer 1989). The outgrowing HMEC (designated as early-passage, $HMEC^{E}$) were heterogeneous and proliferated rapidly for several passages. This stage was followed by a period termed 'selection' when the majority of the cells became larger, flattened, and senescent. The resulting homogeneous population (designated as late-passage, $HMEC^{L}$) could be propagated for another 10-20 passages before senescence (Wazer 1995, Stampfer 1980, Hammond 1984).

Cell culture and transfection- COS-7 (SV40-transformed monkey kidney) and 293 (adenovirus-transformed human kidney) cells were cultured in low-glucose DMEM supplemented with 10% fetal bovine serum. An immortalized human mammary epithelial cell line, 184A1, was maintained in MCDB170 medium (Stampfer 1985). MCF7 cells were grown in MEM supplemented with non-essential amino acids, sodium pyruvate and 10% fetal bovine serum. A primary normal human mammary epithelial cell strain, BE46, and its derivative (E6/BE46) immortalized by the E6 oncogene of HPV16, were cultured in CDM3 medium (Peterson 1987).

Retroviral vectors and packaging cell lines- PA317 cell lines stably expressing HPV-16 E6 (LXSN16E6), HPV-16 E7 (LXSN16E7), or HPV-16 E6 and E7 (LXSN16E6E7) (Halbert 1991) (kindly provided by Dr. D. A. Galloway, Fred Hutchinson Cancer Research Center, Seattle) were grown as described (Halbert 1991). Retroviral vector expressing human E2F-1 was constructed by ligating E2F-1 cDNA (Kaelin 1992) (kindly provided by Dr. William G. Kaelin, Jr. at Dana-Farber Cancer Institute, Boston) into pLXSN vector (Miller 1993) (kindly provided by Dr. A. D. Miller, Fred Hutchinson Cancer Research Center, Seattle) and was introduced into a PA317 amphotropic packaging cell line as previously described (Miller 1993). The viral supernatant from each packaging line was filtered through a 0.45 micron disposable syringe filter and either was used immediately for infections or was frozen on dry ice and stored at -80°C for later use. Viral titers were determined by infection and selection of NIH3T3 cells as previously described (Miller 1993). No production of helper virus was detected by a β–galactosidase mobilization assay (Pear 1993).

Viral infection, selection, and cloning- $HMEC^{E}$ (initial outgrowth) and $HMEC^{L}$ (post-selection) were infected with retrovirus by replacing the medium with diluted virus stocks in the

presence of 4 μg/ml Polybrene (Sigma). After overnight incubation, the supernatant was aspirated and replaced with virus-free DFCI-1 medium. Selection was applied 2 days after infection in medium containing 25 μg/ml G418. For the clonal analysis of infected cells, G418-resistant colonies, which usually emerge within 2 weeks, were isolated using paper cloning disks (PGC Scientific) dipped in trypsin-EDTA solution. These cells were propagated further on Transwell-COL collagen-coated membrane inserts (Coster) which were placed on fibroblast cultures. This culture system supported better growth and cloning efficiency than conventional plastic tissue culture wares (unpublished results).

Telomerase Activity Assay- Telomerase activity was assayed using the telomere-repeat amplification protocol (TRAP) assay (Kim 1994, Wright 1995). Cell extracts were prepared as described (Kim 1994), aliquoted, flash-frozen in liquid nitrogen, and stored at -80°C. Protein concentrations were determined by the Bradford assay (Bio-Rad). An aliquot of each extract was incubated with 12.5 pmol of [^{32}P] 5'-end labeled TS oligonucleotide (Kim 1994) for 30 min at 25°C in 50 μl of a solution containing 10 mM Tris-HCl (pH 8.3), 1.5 mM $MgCl_2$, 50 mM KCl, 0.005% Tween-20, 1 mM EGTA, 50 μM each dNTP, 5 μg of bovine serum albumin and 1 μg of T4 gene 32 protein (Boehringer Mannheim) to allow for elongation of the TS primer by telomerase. The reaction was heated to 94°C before addition of 2 units of Taq polymerase (Boehringer Mannheim) and 12.5 pmol of the CX primer (Kim 1994). The elongated products were amplified by PCR through 30 cycles at 94°C for 30 s, 50°C for 30 s, and 72°C for 90 s. A portion of each PCR product was electrophoresed on a 10% non-denaturing acrylamide gel which was either autoradiographed or scanned with a PhosphorImager (Molecular Dynamics). Extracts were considered negative if no telomerase products were detected after 7 day exposure to Phosphor screens. All extracts that produced 6 bp ladders were tested to confirm sensitivity to RNase treatment, indicative of telomerase activity.

Telomere length analysis- 5 μg of total genomic high molecular weight DNA was digested with restriction enzymes HinfI and RsaI. The digested samples were separated on 0.6 % agarose gel electrophoresis and blotted onto a nylon membrane. A ^{32}P 5'-labeled telomere repeat probe, $(TTAGGG)_6$, was used for Southern analysis under stringent hybridization conditions to detect the telomeric ends.

Western analysis of E2F-1 and c-Myc protein- Total cellular proteins (50 μg /lane) were separated by 10-20 % gradient polyacrylamide gel electrophoresis and were transferred to nitrocellulose membrane as described (Kaelin 1992). The E2F-1 and c-Myc proteins was detected with anti-E2F-1 (C-20) rabbit polyclonal antibody and anti-cMyc monoclonal antibody (Santa Cruz Biotechnology, Inc.), respectively, followed by horseradish peroxidase-conjugated secondary antibody using an ECL system (Amersham).

Matrigel assay- Primary HMEC, BE95 cells, grown on plastic surface were trypsinized, pelleted, washed in PBS, and counted using a Coulter Counter. 2.5 x 10^5 cells were resuspended in 300 μl Matrigel (10 mg/ml, Collaborative Biomedical Products) and plated into a 4-well dish containing a 100 μl Matrigel underlay. These cultures were then incubated at 37°C until Matrigel solidified and then 500 μl of CDM3 growth Media was added. Media was changed every three to four days. Normal HMEC began to form spheroids at day six and cultures were harvested at day ten. These spheroids were approximately 55 μm in diameter and, in the focal plane, some of the cell-cell boundaries can be discerned (Figure 14). Matrigel cultures were washed and fixed in 5%

neutral buffered formalin solution (Sigma). Fixed cultures were embedded in sucrose, frozen in Tissue-Tek OCT compound (VWR), and cut into 5 μm sections. Nuclei were stained with 4,6-diamidino-2-phenylindole (DAPI). Sectionong and DAPI staining of the HMEC sheroids showed the normal ring-like organization of the nuclei surrounding a central luminal space (Figure 14). These sections were then blocked with 10% normal goat serum (Sigma) and goat anti-mouse Fab fragment (Jackson ImmunoResearch Laboratories, Inc) and then used for indirect immunodluorescence staining. Antibodies used were: E-cadherin (mouse Ig2a, 36) 1:100 dilution (Transduction Laboratories), type IV collagen (mouse IgG1, CIV 22) 1:50 dilution (DAKO), lactoferrin (rabit sera) 1:50 dilution (Zymed), cytokeratin 19 (mouse IgG1, RCK 108) 1:100 dilution (DAKO), goat anti-mouse Ig2a-Texas Red, 1:200 dilution, goat anti-rabbit-Texas Red, 1:200 dilution (Accurate Chemical and Scientific) and goat anti-mouse IgG1- FITC, 1:200 dilution (Southern Biotechnology Associates). The images were then captured using a CCD camera/the Vysis/SmartCapture Cell Imaging System.

Immunofluorescence Microscopy- Cells were grown to exponential phase in glass chamber slides and fixed in 2% neutral paraformaldehyde in PBS for 30 min on ice, then permeabilized in 0.2% Triton X-100 in TBS (10 mM Tris, pH 7.5, 150 mM NaCl, 1 mM KCl) for 10 min at room temperature or fixed in cold methanol for 5 min. All antibodies were diluted in TBS with 0.1% Triton X-100, 1% BSA and 3% goat serum. Incubation with primary antibody was carried out for 1 hr at room temperature. After three washes with TBS, incubation with secondary antibody was carried out for 30 min at room temperature, followed by staining of DNA with 4', 6'-diamidino-2-phenylindole (DAPI) for 5-10 min. Slides were mounted with Antifade (Molecular Probes) after three washes in TBS, and examined with a fluorescence microscope (Zeiss) under the 100X objective. Color slides were taken using Kodak Ektachrome 400 film. Primary antibodies for these experiments included BRCA1 MS110 (1:100 dilution, mouse IgG1, Calbiochem Ab-1); BRCA1 C-20 (1:100, rabbit polyclonal IgG, Santa Cruz); γ-tubulin GTU-88 (1:2000, mouse IgG1, Sigma); α-tubulin DM1A (1:1000, mouse IgG1, ICN); and pericentrin 4B (1:500, rabbit polyclonal, a gift from Dr. S. Doxsey). Secondary antibodies included affinity-purified and human serum-adsorbed fluorescein isothiocyanate (FITC)-conjugated goat anti-mouse IgG (Southern Biotechnology Associates) and Texas Red-conjugated AffiniPure goat anti-rabbit IgG (Accurate Chemical & Scientific Corporation). Secondary antibodies were used at final dilutions of 1:200 to 1:400.

Centrosome Isolation and Western Analysis- Isolation of centrosomes was based on a method developed by Moudjou and Bornens (1994). Exponentially growing COS-7 or MCF7 cells were incubated with culture medium containing 1 μg/ml cytochalasin D and 0.2 μM nocodazole for one hour at 37°C, to depolymerize actin and microtubule filaments. Cells were then harvested by trypsinization and lysed in a solution of 1 mM Hepes (pH 7.2), 0.5% NP-40, 0.5 mM MgCl2, 0.1% β-mercaptoethanol with proteinase inhibitors (EDTA-free proteinase inhibitor cocktail, Boehringer-Mannheim) and phosphatase inhibitors (50 mM sodium fluoride, 1 mM sodium orthovanadate). Swollen nuclei and chromatin aggregates were removed by centrifugation at 2500 x g for 10 min, and the supernatant was filtered through a 50-μm nylon mesh. Hepes was adjusted to 10 mM, DNase I (Boehringer-Mannheim) was added to 2 units /ml, and the mixture was incubated for 30 min on ice. The lysate was then underlaid with 60% sucrose solution (60% w/w sucrose in 10 mM Pipes, pH 7.2, 0.1% Triton X-100, and 0.1% β-mercaptoethanol). Centrosomes were sedimented into the sucrose cushion by centrifugation at 10,000 x g for 30 min. This crude centrosome preparation was purified further by discontinuous sucrose gradient centrifugation at 120,000 x g for

1 hr. Usually 1-3 x 10^7 cells were lysed in 5 ml of lysis buffer, and the cushion consisted of 0.5 ml of 60% sucrose. After centrifugation, 1.5 ml from the bottom layer was resuspended and loaded onto a discontinuous gradient consisting of 500 µl of 70%, 300 µl of 50% and 300 µl of 40% sucrose solutions. Fractions were collected from the bottom, 200 µl per fraction, from fractions 1 to 7; the remaining solution (~1 ml) was collected as fraction 8. Each fraction was diluted in 1 ml of 10 mM Pipes buffer, pH 7.2. Centrosomes were recovered by centrifugation at 15000 rpm for 10 min in a microfuge and denatured in SDS sample buffer (62.5 mM Tris, pH 6.8, 10% glycerol, 2% SDS, 1.4% β-mercaptoethanol, 0.001% bromophenol blue). Whole cell lysates (WCLs) were prepared by sonicating cells briefly in RIPA buffer (50 mM Tris, pH 8.0, 150 mM NaCl, 0.1% SDS, 0.1% sodium deoxycholate, 1% NP-40) with proteinase and phosphatase inhibitors, followed by centrifugation at 13000 rpm for 10 min in a microfuge to remove cell debris, and denatured in SDS sample buffer. Proteins were separated by 4-15% SDS-polyacrylamide gel electrophoresis (SDS-PAGE) and transferred to nitrocellulose membranes. Membranes were blocked in 100 mM Tris, pH 7.5, 150 mM NaCl, 0.1% Tween 20 (TBST) with 2% dry milk for 30 min at room temperature. Primary and secondary antibody hybridizations were carried out in TBST with 2% dry milk for 30-60 min; membranes were washed in TBST. Signals were detected using ECL (Amersham or Pierce). Primary antibodies for these experiments included (i) BRCA1 MS110 (mouse IgG1, 1:5 dilution, a gift from Dr. R. Scully or 1:50 dilution, Calbiochem Ab-1); (ii) BRCA1 MS13 (1:50, mouse IgG1, Calbiochem Ab-2); (iii) BRCA1 D-20 (1:50, rabbit polyclonal IgG, Santa Cruz); (iv) γ-tubulin GTU-88 (1:10,000, mouse IgG1, Sigma); (v) α-tubulin DM1A (1:250, mouse IgG1, ICN); (vi) cyclin B (1:1000, mouse IgG1, Transduction Laboratories); (vii) $p34^{cdc2}$ (1:1000, mouse IgG1, Transduction Laboratories); and (viii) lamin X67 and X233 (1:40, mouse IgG1, American Research Products). The secondary antibody was horseradish peroxidase-conjugated goat anti-mouse or anti-rabbit (Pierce).

Flow Cytometry- Cells were trypsinized and resuspended in ice-cold PBS (devoid of magnesium and calcium ions) at a density of 1-2 x 10^6/ml, fixed by adding 2 ml ice-cold methanol per ml of cells in PBS with vortexing, and incubated at least 30 min on ice. Cells were collected by centrifugation at 1000 x g, resuspended in a solution containing 0.5 ml of propidium iodide and 0.5 ml of ribonuclease A (200 U/ml), and incubated at least 30 min at room temperature before analysis by flow cytometry.

Immunoprecipitation- Cells were lysed in PBS with 0.1% NP-40, 0.1% Triton X-100, protease inhibitors (20 µg/ml aprotinin, 10 µg/ml leupeptin, 1 mM PMSF and 1 µg/ml pepstatin A) and phosphatase inhibitors (50 mM sodium fluoride, 1 mM sodium orthovanadate), and sonicated briefly. Lysates cleared by centrifugation at 13000 rpm for 15 min were incubated with 3 µg of BRCA1 C-20 with or without 20 µg of C-20 peptide; or incubated with 7-14 µg of γ-tubulin antibody for 30 min on ice. Either protein A-Sepharose or protein G-agarose (Sigma) was added and the incubation was continued for 1-2 h at 4°C. Samples were washed four times with the lysis buffer, denatured in SDS sample buffer, fractionated on 6% or 4-12% SDS-polyacrylamide gels, and blotted to nitrocellulose membranes. Western hybridization was performed as described above. MS110 was used to detect immunoprecipitated BRCA1; γ-tubulin was detected by the same antibody used for immunoprecipitation. *In vitro* transcription and translation of full-length BRCA1 were carried out using a kit from Promega and BRCA1 cDNA in pCR-Script (a gift from Dr. Jeff Holt) as template.

Table 1. Breast Tissue Samples (shown here are from BE-1 to BE-94).

BE-1	mastectomy
BE-2	BRCA-1 mastectomy
BE-3	mastectomy
BE-4	mastectomy
BE-5	mastectomy
BE-6	mastectomy
BE-7	mastectomy
BE-8	mastectomy
BE-9	mastectomy
BE-10	mastectomy
BE-11	mastectomy
BE-12	mastectomy
BE-13	mastectomy
BE-14	mastectomy
BE-15	punch biopsy
BE-16	mastectomy
BE-17	mastectomy
BE-18	mastectomy
BE-19	mastectomy
BE-20	NF-1 mastectomy
BE-21	APC biopsy
BE-22	mastectomy
BE-23	mastectomy
BE-24	mastecto;my
BE-25	NF-1 biopsy
BE-26	APC biopsy
BE-27	mastectomy
BE-28	mastectomy
BE-29	mastectomy
BE-30	mastectomy
BE-31	reduction mammoplasty
BE-32	reduction mammoplasty
BE-33	APC mastectomy
BE-34	APC mammotest biopsy
BE-35	fine-needle biopsy
BE-36	fine-needle biopsy
BE-37	fine-needle biopsy
BE-38	fine-needle biopsy
BE-39	fine-needle biopsy
BE-40	BRCA-1 mammotest biopsy
BE-41	mastectomy
BE-42	fine-needle biopsy
BE-43	fine-needle biopsy
BE-44	APC mammotest
BE-45	bilateral mastectomy
BE-46	reduction mammoplasty
BE-47	reduction mammoplasty
BE-48	mastectomy
BE-49	reduction mammoplasty
BE-50	reduction mammoplasty
BE-51	mastectomy
BE-52	mastectomy
BE-53	mastectomy
BE-54	reduction mammoplasty
BE-55	APC mammotest biopsy
BE-56	APC mammotest biopsy
BE-57	APC mammotest biopsy
BE-58	APC mammotest biopsy
BE-59	BRCA-1 mammotest biopsy
BE-60	prophylactic mastectomy
BE-61	mastectomy
BE-62	mastectomy
BE-63	mastectomy
BE-64	biopsy
BE-65	biopsy
BE-66	mastectomy
BE-67	mastectomy
BE-68	reduction mammoplasty
BE-69	mastectomy
BE-70	bilateral mastectomy
BE-71	mastectomy
BE-72	BRCA-1 mammotest
BE-73	mastectomy
BE-74	mastectomy
BE-75	BRCA-1 mammotest
BE-76	reduction mammoplasty
BE-77	BRCA-2 mastectomy
BE-78	mastectomy
BE-79	mastectomy
BE-80	APC mammotest biopsy
BE-81	mastectomy
BE-82	reduction mammoplasty
BE-83	mastectomy
BE-84	reduction mammoplasty
BE-85	reduction mammoplasty
BE-86	reduction mammoplasty
BE-87	mastectomy
BE-88	mastectomy - high risk
BE-89	mastectomy
BE-90	reduction mammoplasty
BE-91	biopsy - high risk
BE-92	mastectomy - high risk
BE-93	mastectomy
BE-94	bilateral mastectomy

Table 2. Immunofluorescence staining of Bcl-2, cytokeratin 19 (K19), and vimentin in BE46 and pLNPObcl-2/BE46. '+' is an indicator if the intensity of staining. Numbers in parenthesis indicate the estimated percentages of positive staining cells.

	BE46	pLNPObcl-2/BE46
Bcl-2	±	+++ (>90%)
K19	+++ (90-100%)	++ (<10%)
Vimentin	++ (10-20%)	+++ (50-70%)

Table 3. Doxycyclin (DOX) repression of LINX GFP in infected breast cancer lines as determined by FACS analysis.

To test the efficacy of the tetracycline repressible LINX vector system, GFP was cloned into the LINX vector. Shown here are the results of the addition of DOX to LINX-GFP infected breast cancer cell lines. The effect of DOX suppression is clearly visible after four days of incubation and after eight days incubation, the fluorescent signal is reduced to a small percentage of the original. The GFP signal detected at the eight day mark could be caused either by incomplete suppression of the Tet repressor; alternatively it may be that the signal is residual and results from the slow turn-over rate of the highly stable GFP protein.

Breast Cancer Cell line	Cell-type specific autofluorescence with LINX vector alone	% Cells fluorescent following LINX-GFP infection	Mean Fluorescence Intensity following LINX-GFP infection	Mean Fluorescence Intensity 4 Days after DOX addition	Mean Fluorescence Intensity 8 Days after DOX addition	Residual GFP after eight days of incubation with DOX
MCF7	1.65	76.04	228	90	15	6.6%
BT549	2.02	85.32	629	294	28	4.5%
MDA-MB468	1.82	76.86	599	323	56	9.3%

Table 4.

	Image ID	Clone definition
1	358433	Human retinoid X receptor-gamma mRNA, complete cds
2	295401	ESTs
3	1088345	S100 calcium-binding protein A7 (psoriasin 1)
4	276282	ESTs
5	269017	Human O-linked GlcNAc transferase mRNA, complete cds
6	545239	Neutrophil Gelatinase-Associated Lipocalin Precursor
7	882141	DNA G/T mismatch-binding protein
8	283063	MHC class II DQ-beta associated with DR2, DQw1 protein
9	156431	Ciliary neurotrophic factor receptor
10	770435	Transcription factor p65
11	700466	
12	277134	ESTs
13	275272	ESTs
14	273039	ESTs
15	283618	ESTs
16	23240	SM22-alpha homolog
17	627104	Human alpha-tubulin mRNA, complete cds
18	33934	ESTs
19	610187	Proteasome Component C9
20	592947	Autoantigen PM-SCL
21	46743	ESTs, Highly similar to RAS-related protein RAP-1B
22	23904	ESTs
23	264369	ESTs, Highly similar to GLUCOSYLTRANSFERASE ALG8
24	200531	ESTs
25	126783	ESTs
26	201891	ESTs
27	265684	ESTs
28	261971	Metallopeptidase 1 (33 kD)
29	129503	ESTs

The genes listed in this table showed 3× fold or more variation in expression levels in a comparison between primary human mammary cells, with and without induced β-catenin.

Table 5.

Color	Clone definition
green	IK
red	INTERFERON-ALPHA INDUCED 11.5 KD PROTEIN
green	SERUM AMYLOID A PROTEIN PRECURSOR
green	Protein tyrosine phosphatase, receptor type, f polypeptide
green	ESTs
red	PROTEASOME COMPONENT C13 PRECURSOR
green	Epidermal growth factor receptor
red	Human effector cell protease receptor-1 (EPR-1) gene, partial cds
red	Glyceraldehyde-3-phosphate dehydrogenase
green	Oxytocin receptor
green	Sterol carrier protein 2
green	Oxytocin receptor
green	Superoxide dismutase 2, mitochondrial
green	Insulin-like growth factor 1 (somatomedia C)
green	Ribosomal protein S6 kinase, 90kD, polypeptide 2
green	S100 calcium-binding protein A8 (calgranulin A)
red	Laminin receptor (2H5 epitope)
red	ESTs, Moderately similar to hPMSR2 [H.sapiens]
green	Cell division cycle 42 (GTP-binding protein, 25kD)
red	ESTs
green	ESTs, Weakly similar to similar to deoxyribose-phosphate aldolase
red	Glyceraldehyde-3-phosphate dehydrogenase
green	Human mRNA for KIAA0208 gene, complete cds
green	Protein tyrosine phosphatase, receptor type, alpha polypeptide
red	H.sapiens mRNS for clathrin-associated protein
green	Major histocompatibility complex, class I, C
red	SRF accessory protein 1B (SAP-1)

The genes listed in this table showed 3× fold or more variation in expression levels in a comparison between human mammary epithelial cells, with E6 (green) and with E6/E7 (red).

FIGURES

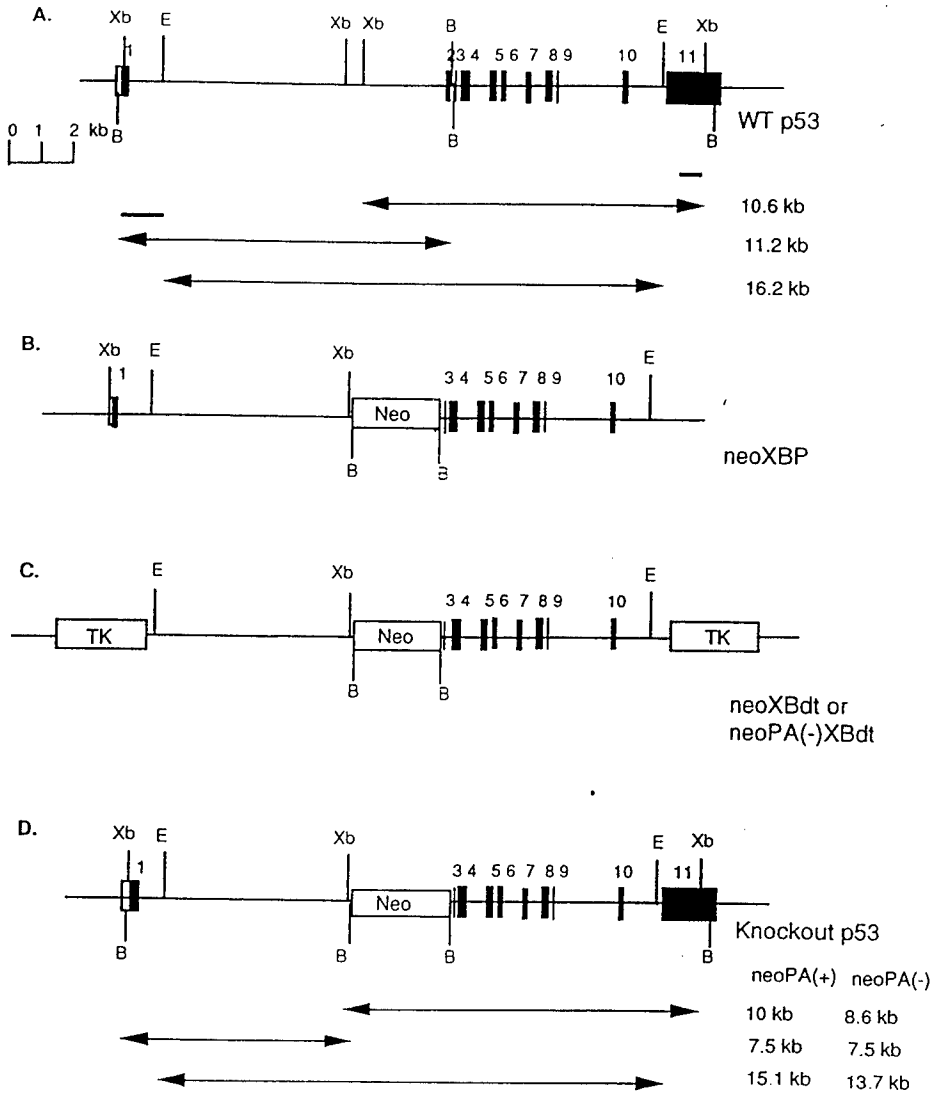

Figure 1. Genomic map of the *p53* gene (A), the *p53* knockout constructs: neoXBP (B), neoXBdt or neoPA(-)XBdt (C), and the *p53* knockout allele (D). Sizes of predicted DNA fragments from XbaI, BamHI or EcoRI digestion are indicated on the right. A SmaI-XbaI cDNA fragment from Exon 11 is used as a probe for XbaI digests. An XbaI-EcoRI DNA fragment from exon 1 and intron 1 is used as the probe for BamHI digests. Both sequences are flanking the sequences used for the construction of knockout vectors, therefore, can detect wildtype and knockout alleles only. *p53* cDNA probe is used to detect EcoRI digested DNA. B, BamHI; E, EcoRI; Xb, XbaI.

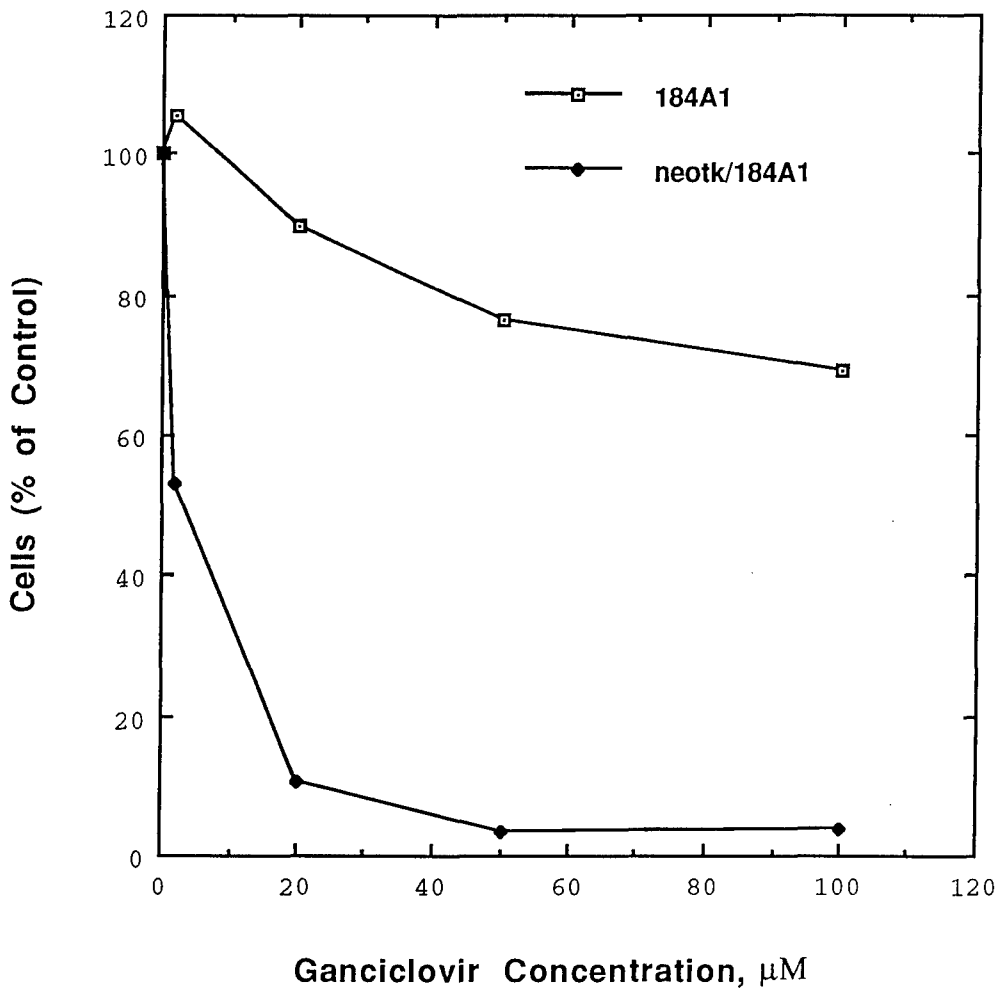

Figure 2. The effect of ganciclovir on cell growth of 184A1 and HSV-*tk*-transfected 184A1. Cell numbers in dishes with no ganciclovir were used as controls (100%).

Figure 3. Telomerase activity in pre- and post-crisis HMEC transduced with HPV-16 oncogenes. HMEC^{E} (initial outgrowth, passage 1) and HMEC^{L} (post-selection, passage 8) infected with retrovirus expressing HPV-16 E6, E7, E6E7, or vector control were cultured in medium containing 25 μg/ml G418. HMEC^{E} transduced by vector control or E6 senesced within 10 passages after virus infection, although E6-transduced HMEC^{E} occasionally produced a few immortal clones in some experiments. HMEC^{L} transduced by vector control or E7 senesced within 6 passages. E7-transduced HMEC^{E}, E6E7-transduced HMEC^{E}, E6-transduced HMEC^{L}, and E6E7-transduced HMEC^{L} went into crisis at passage 14, 10, 15, and 16, respectively, and thereafter became immortal. The cell extracts were prepared at indicated passage (P) number and then subjected to the TRAP assay, using 1 μg of protein.

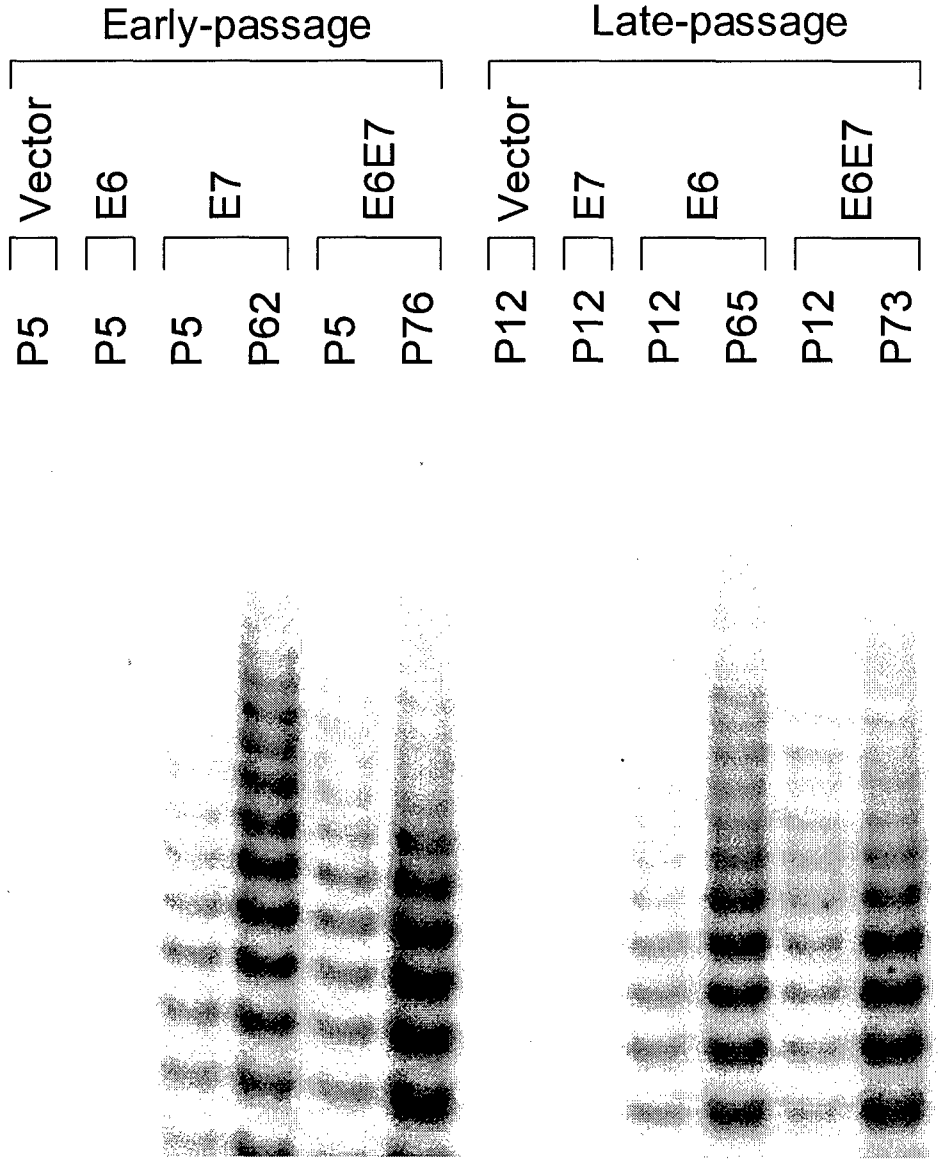

Figure 4. Telomerase activation in HMEC^{E} and HMEC^{L} by E7 or E6. HMEC^{E} and HMEC^{L} were plated in six-well polystyrene tissue culture dishes at approximately 10% confluency. Cells were incubated overnight with virus stocks of vector control, E6, E7, or E6E7 constructs at a multiplicity of infection of 10. Cells were cultured without G418 selection and became confluent by 8 days after infection. Cell extracts were prepared at 2, 4, and 8 days after infection and the amounts shown were subjected to the TRAP assay.

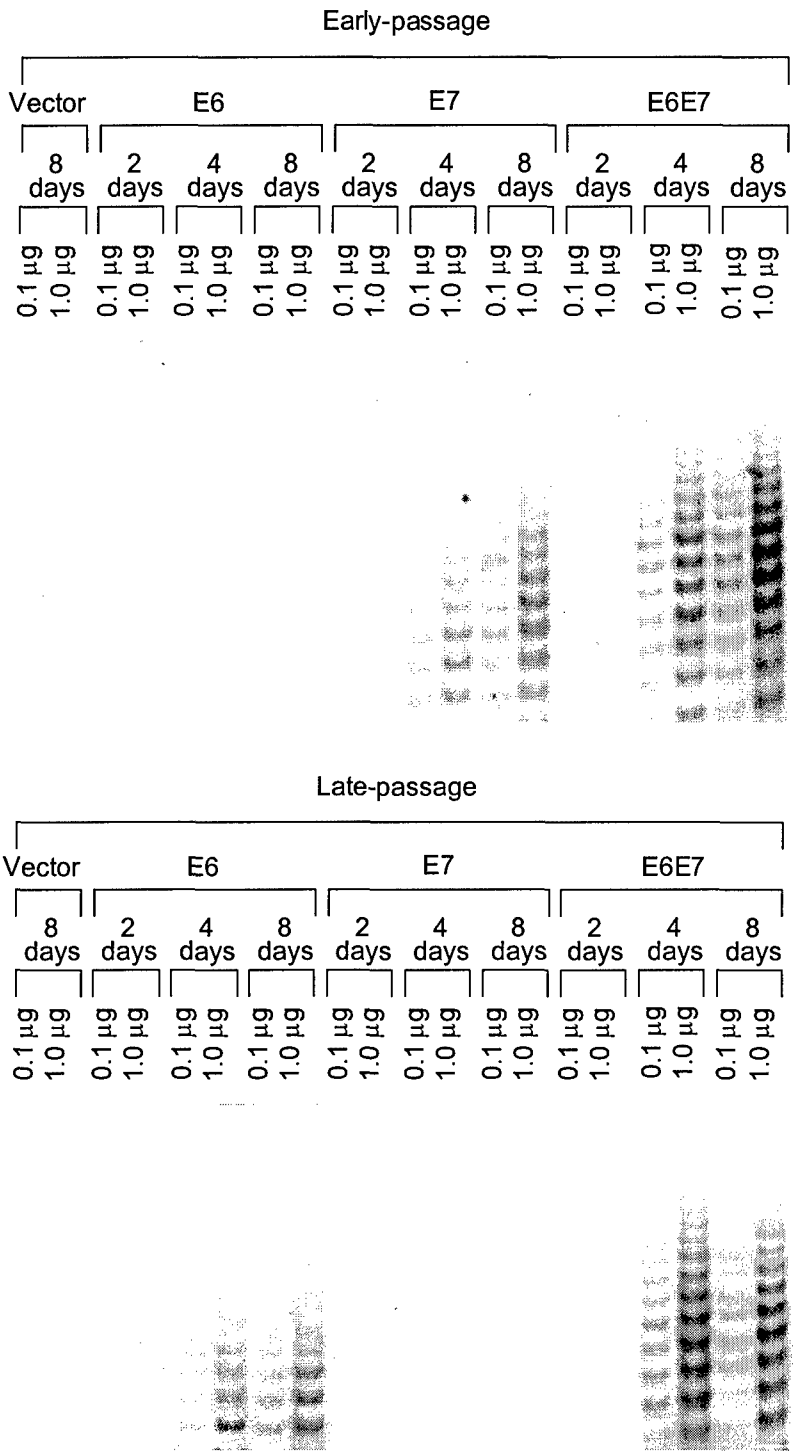

Figure 5. Clonal analysis of E7-transduced HMEC^{E}. A. G418 resistant colonies were isolated two weeks after transduction of E7 into HMEC^{E}, as described in Methods. Half of the cells from each dish were used to prepare a cell extract at passage (4 weeks after infection), and the remaining cells were split ¼, distributed over 4 dishes; again grown to confluence, split ¼ and distributed over 16 dishes and incubated (again, approximately 4 weeks). Those dishes that produced growing cells were cultured further to determine the life span of the cells that grew out. Of sixteen clones, ten senesced during the next several passages (termed S1-S12) and four yielded immortalized progeny (termed Im1-Im4). The corresponding cell extracts prepared earlier were subjected to the TRAP assay. B. TRAP activity was quantified using ImageQuant software (Molecular Dynamics). The results represent the means ± S.D. of two TRAP assay experiments.

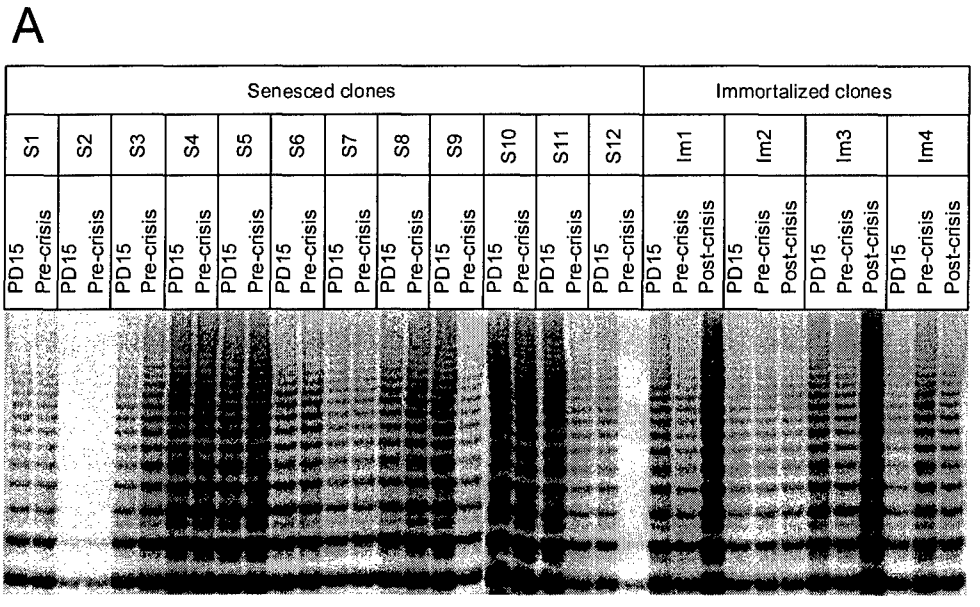

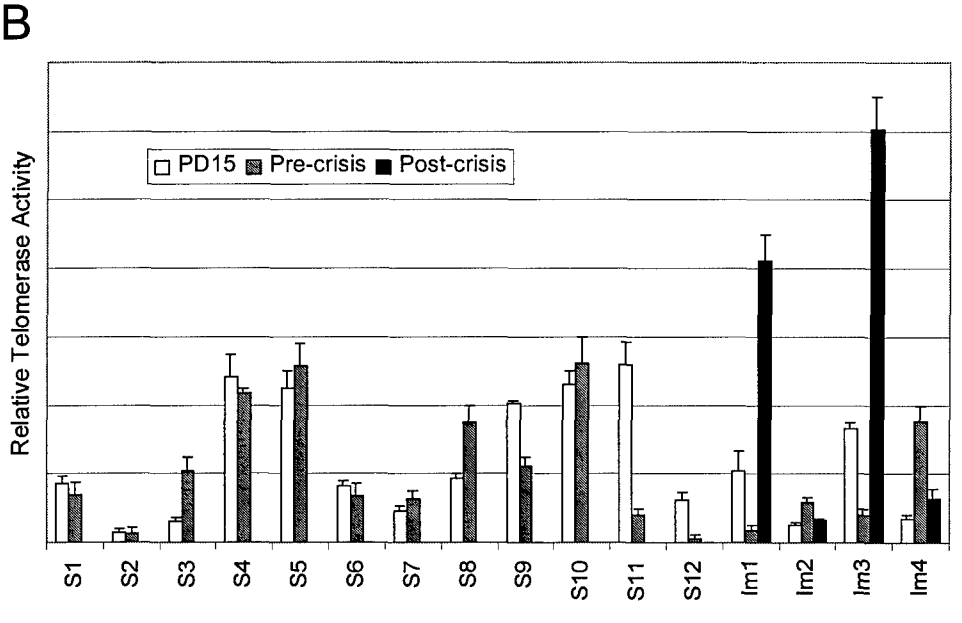

Figure 6. Telomere length in E7-transduced HMEC^{E} at passage 1, at crisis and after immortalization. Total genomic high molecular weight DNA samples prepared from E7-transduced HMEC^{E} at passage 1 and at crisis and from E7-immortalized HMEC^{E} clones (Im1-4) were digested with HinfI and RsaI. The digested samples were subjected to Southern analysis using a ^{32}P 5'-labeled telomere repeat probe, $(TTAGGG)_6$. The average telomere length decreased from approximately 9 to 6.5 kb between passage 1 and crisis. All immortalized clones (Im1-4) showed even shorter average telomere length (4.5-5.5 kb).

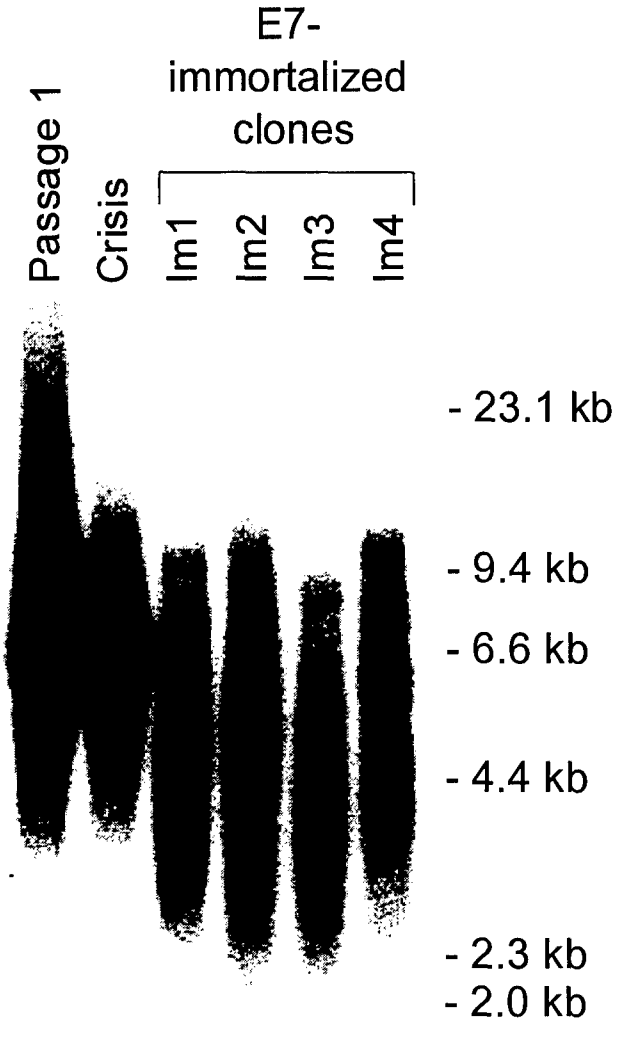

Figure 7. Telomerase activation and c-Myc protein induction by E2F-1. A. Western analysis of cell extracts from HMEC^{E} infected with either vector alone or E2F-1 expressing construct. Total cellular proteins (50 μg /lane) were separated by 10-20 % gradient polyacrylamide gel electrophoresis and were transferred to nitrocellulose membrane. The E2F-1 protein was detected with anti-E2F-1 (C-20) rabbit polyclonal antibody (Santa Cruz Biotechnology, Inc.) and horseradish peroxidase-goat anti-rabbit IgG using an ECL system (Amersham). B. Telomerase activation by E2F-1 overexpression. The cell extracts were prepared from indicated HMEC after each infection and the amount shown were subjected to the TRAP assay. C. Western analysis for c-Myc protein.

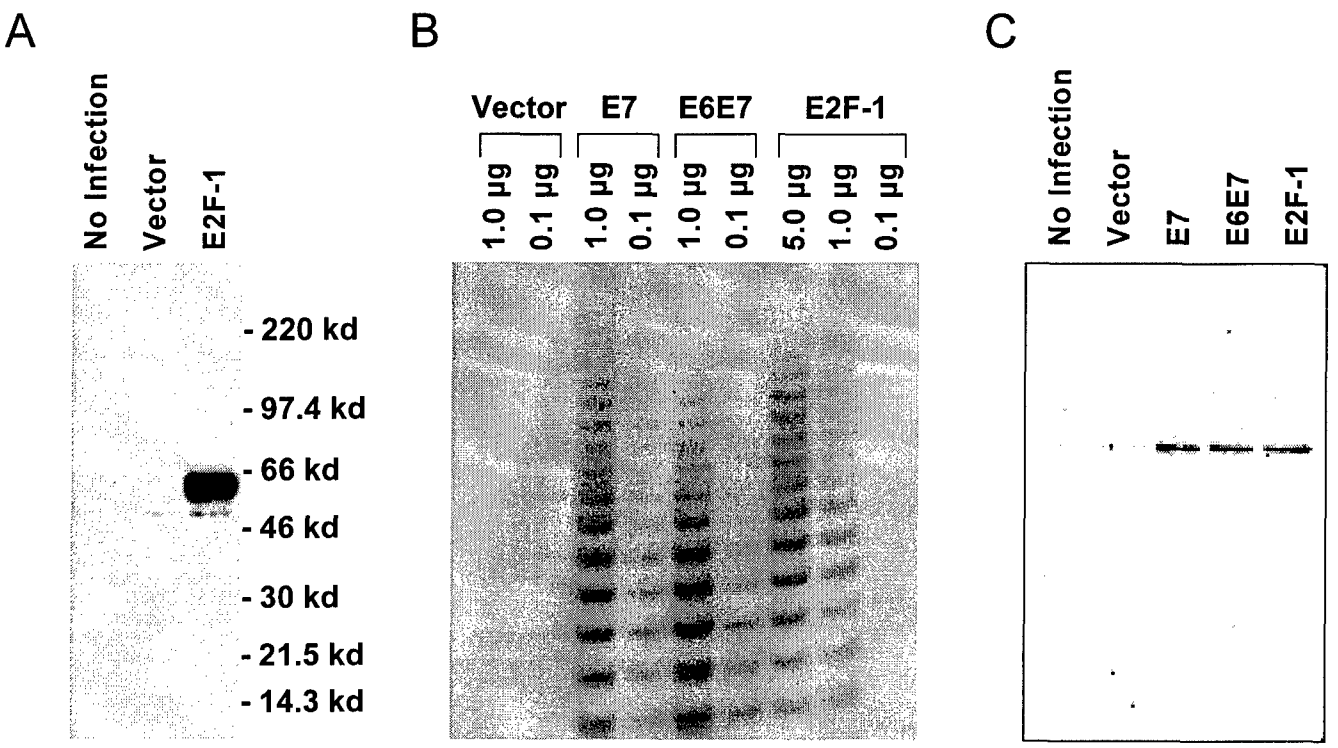

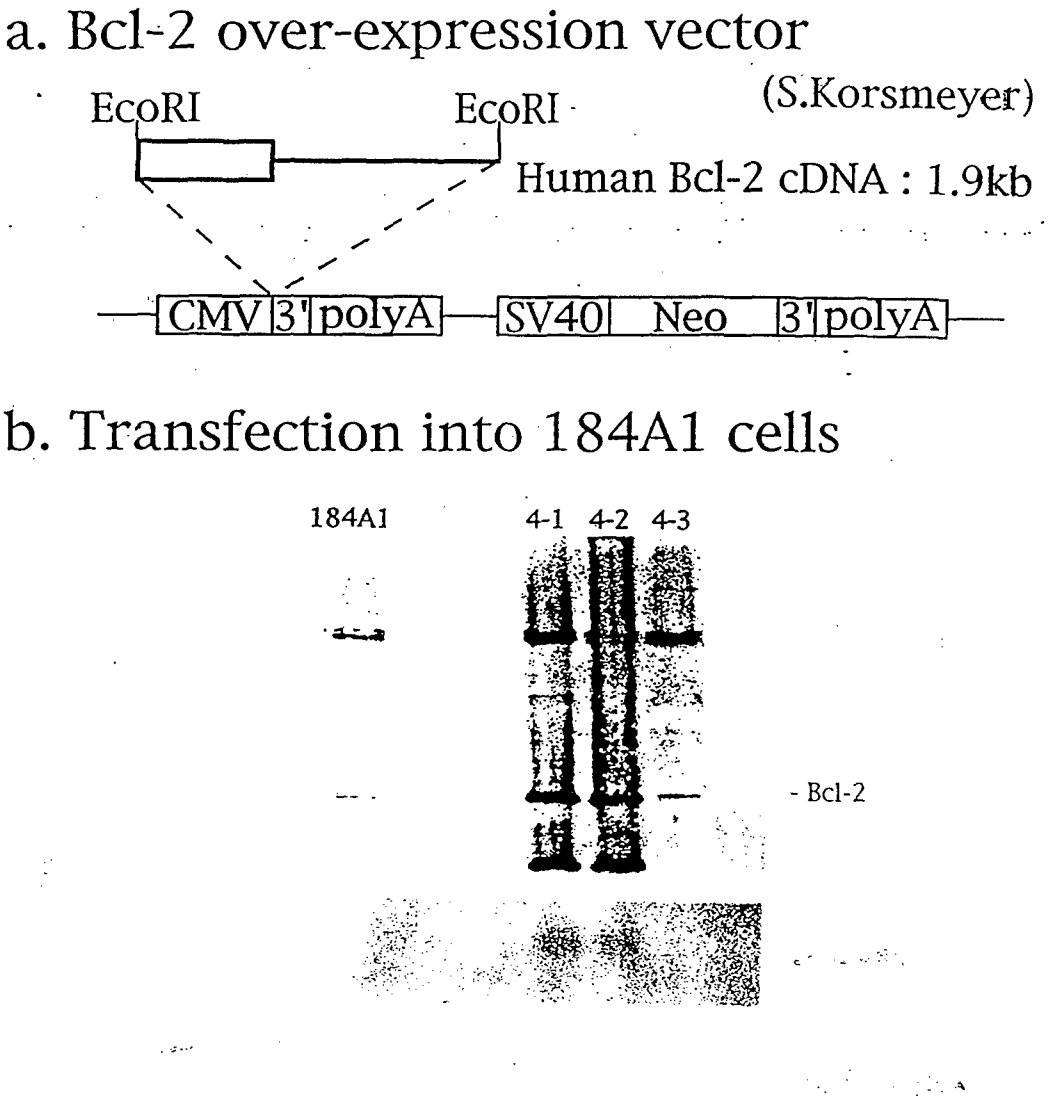

Figure 8 a) The bcl-2 expression vector, pCMVhubcl-2-neo; b) Western (upper panel) and Northern (lower panel) analyses of 184A1 and pCMVhubcl-2-neo-transfected 184A1 cell clones, 4-1, 4-2, and 4-3.

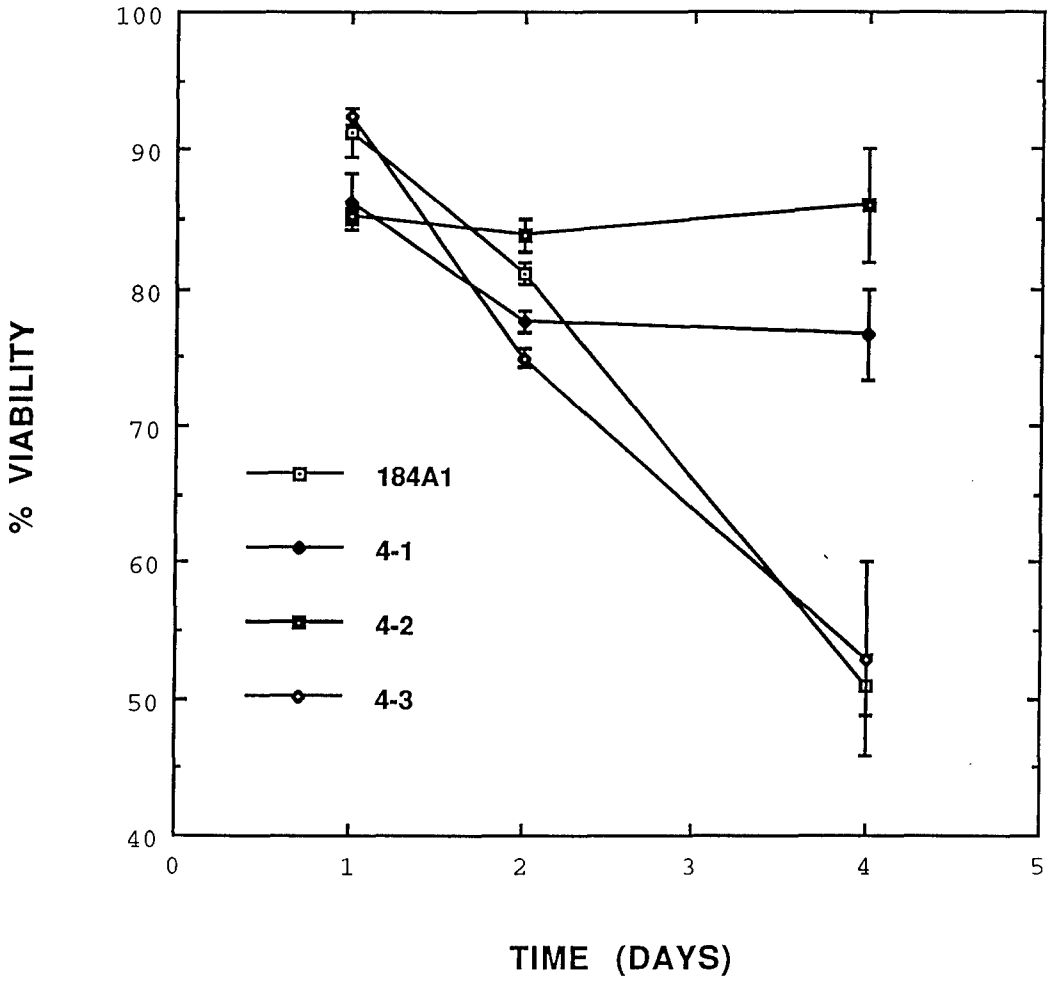

Figure 9 Cell viability of 184A1 and pCMVhubcl-2-neo-transfected 184A1 cell clones, 4-1, 4-2, and 4-3.

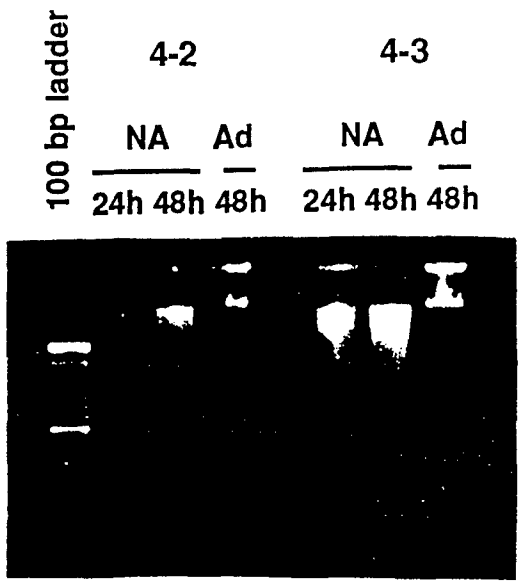

Figure 10. DNA fragmentation analysis of pCMVhubcl-2-neo-transfected 184A1 cell clones, 4-2 and 4-3. 'NA' indicates nonadherent, and 'Ad' indicates adherent cells.

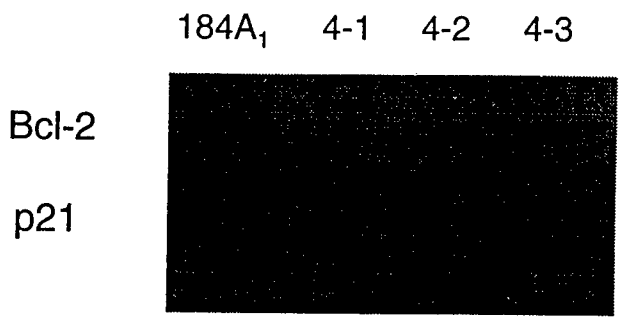

Figure 11. Western analysis of Bcl-2 and p21 *WAF-1*.

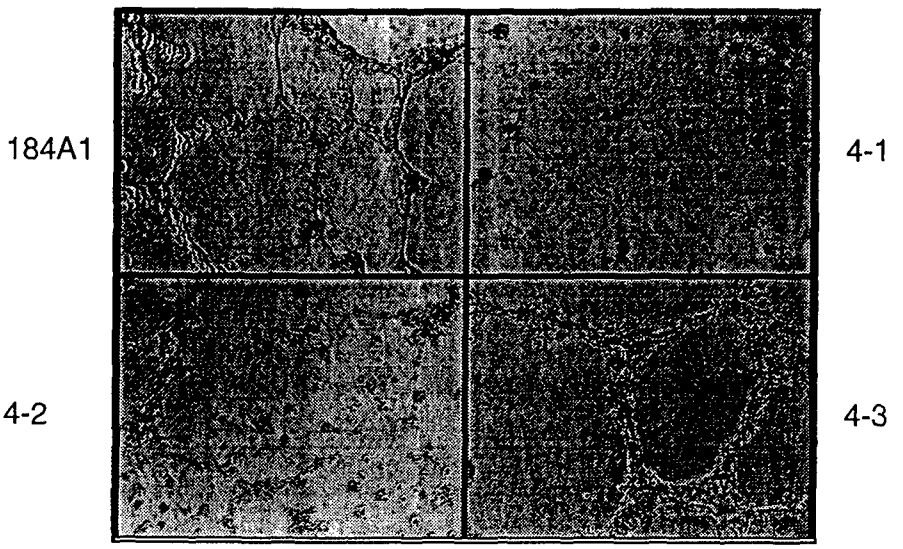

Figure 12. Structure formation of 184A1 cell clones on Matrigel.

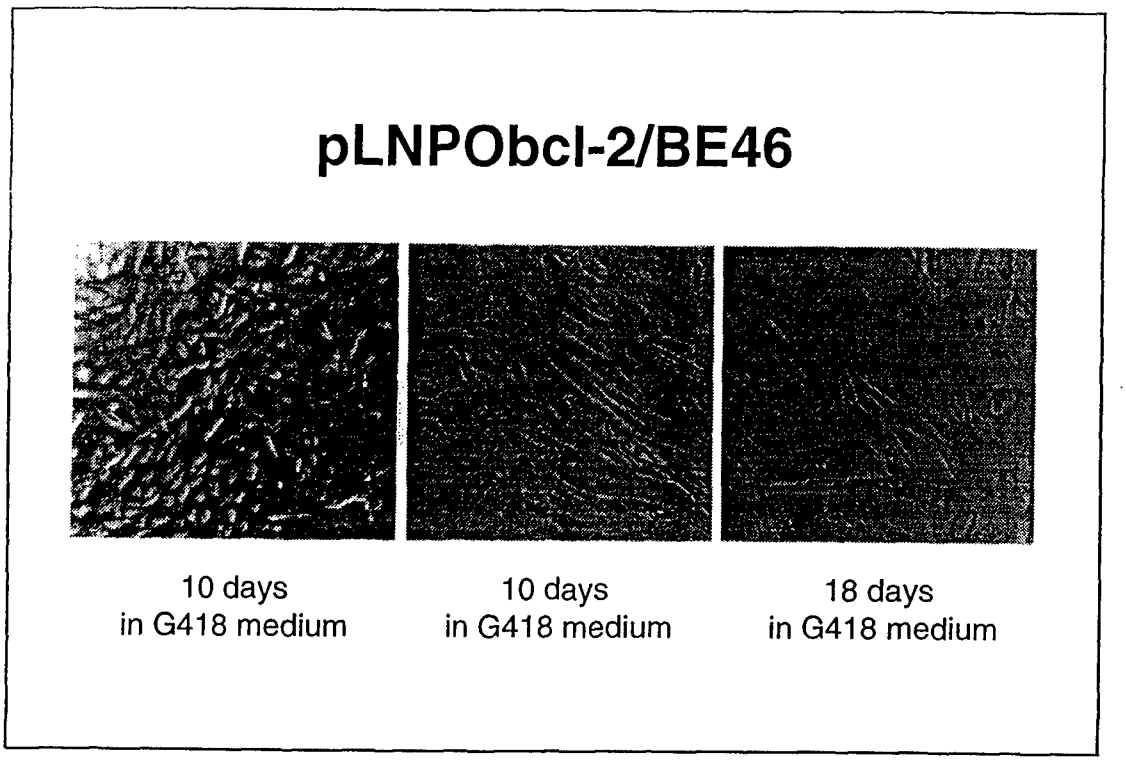

Figure 13.Morphology of pLNPObcl-2/BE46. Ten and 18 days in G418 selecting medium.

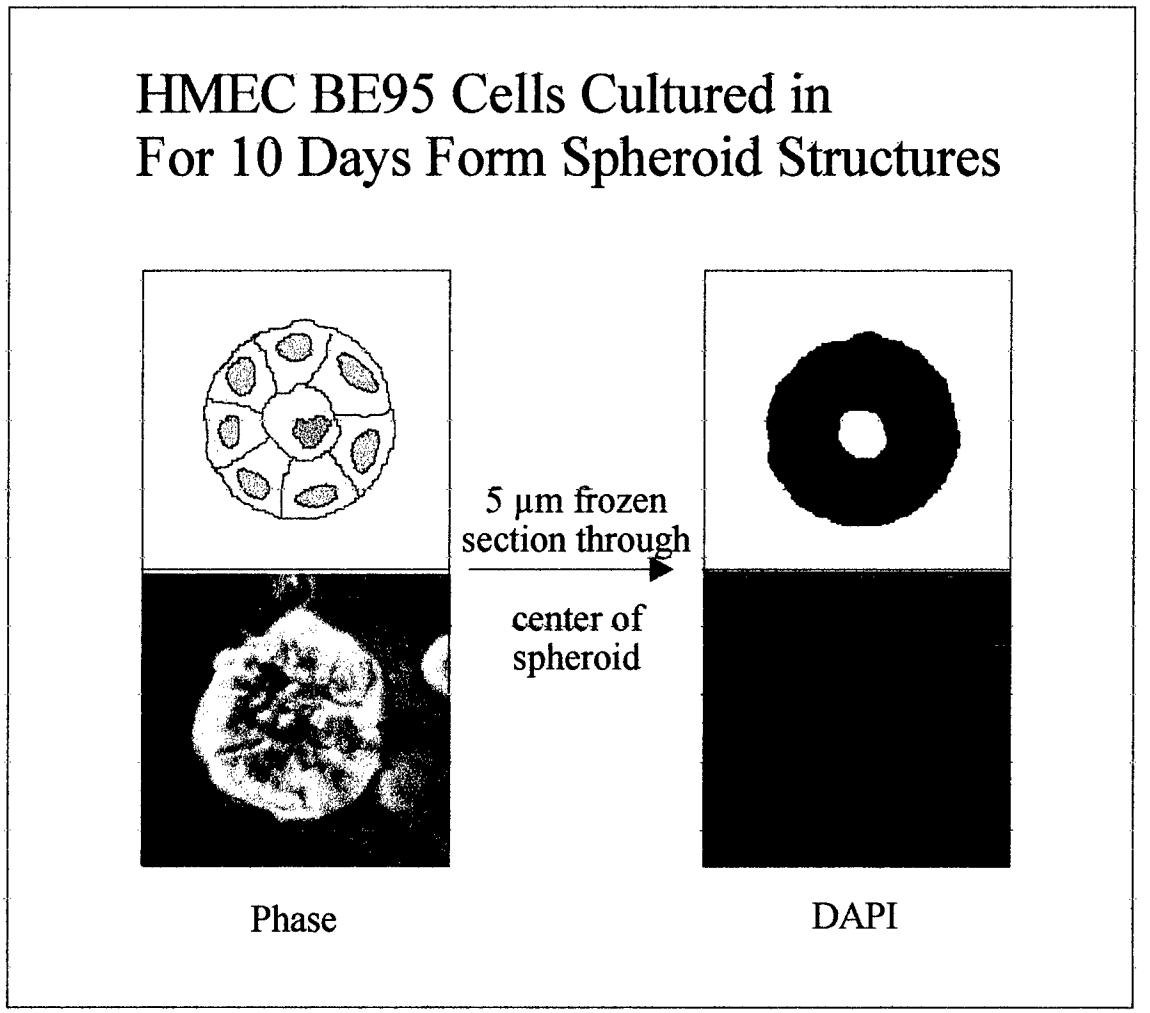

Figure 14. Primary BE95 cells cultured in Matrigel for 10 days formed spheroids . Normal HMEC, BE95 cells, grown on plastic were trypsinized and resuspended in liquid Matrigel as single cells. Luminal cell spheroids were approximately 55 micrometers in diameter. These Matrigel cultures were fixed with formalin and frozen in O.C.T. (Tissue-Tek®). Frozen cultuers were sectioned and nuclei were stained with 4,6-diamidino-2-phenylindole (DAPI). This example shows a ring of seven cells surrounding a luminal space.

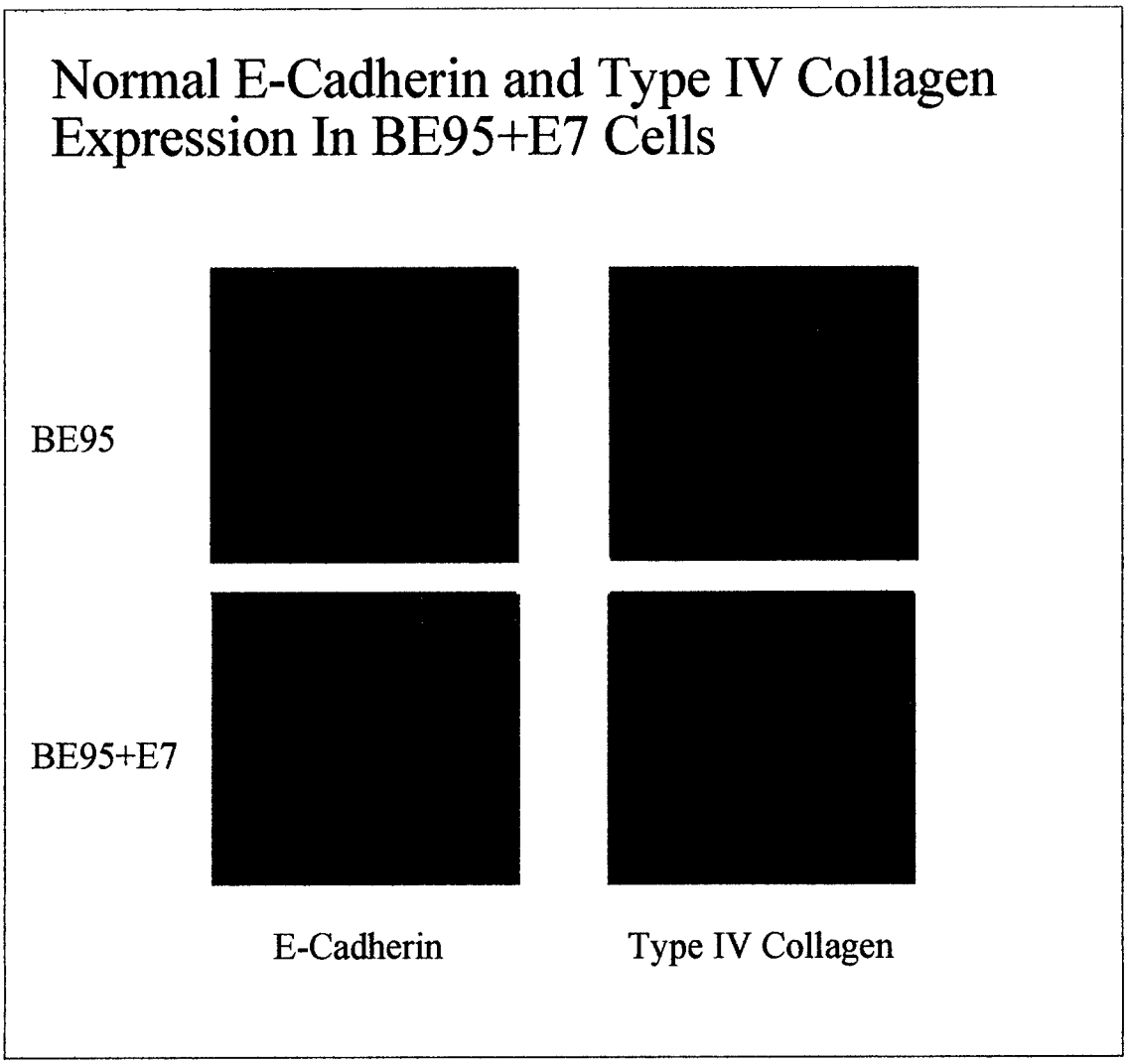

Figure 15. BE95+E7 cultures show a normal staining pattern for E-Cadherin and type IV collagen. E-Cadherin is a cell-cell adhesion marker and it is present at points of cell-cell contact in both the BE95 and BE95+E7 cells. Additionally, both cell types basally deposit a continuous type IV collagen-containing basement membrane. Day ten Matrigel cultures were fixed, frozen, and cut into five micrometer
sections. These sections were then used for indirect immunofluorescence. Antibodies were used in the following concentrations: E-Cadherin (mouse IgG2a, 36) 1:100 (Transduction Laboratories), collagen IV (mouse IgG1, CIV 22) 1:50 (DAKO), goat anti-mouse IgG2a-Texas Red and goat anti-mouse IgG1-fluorescein isothiocyanate 1:200 (Southern Biotechnology Associates). These images were captured using a CCD camera and the Vysis/Smart Capture Cell Imaging System.

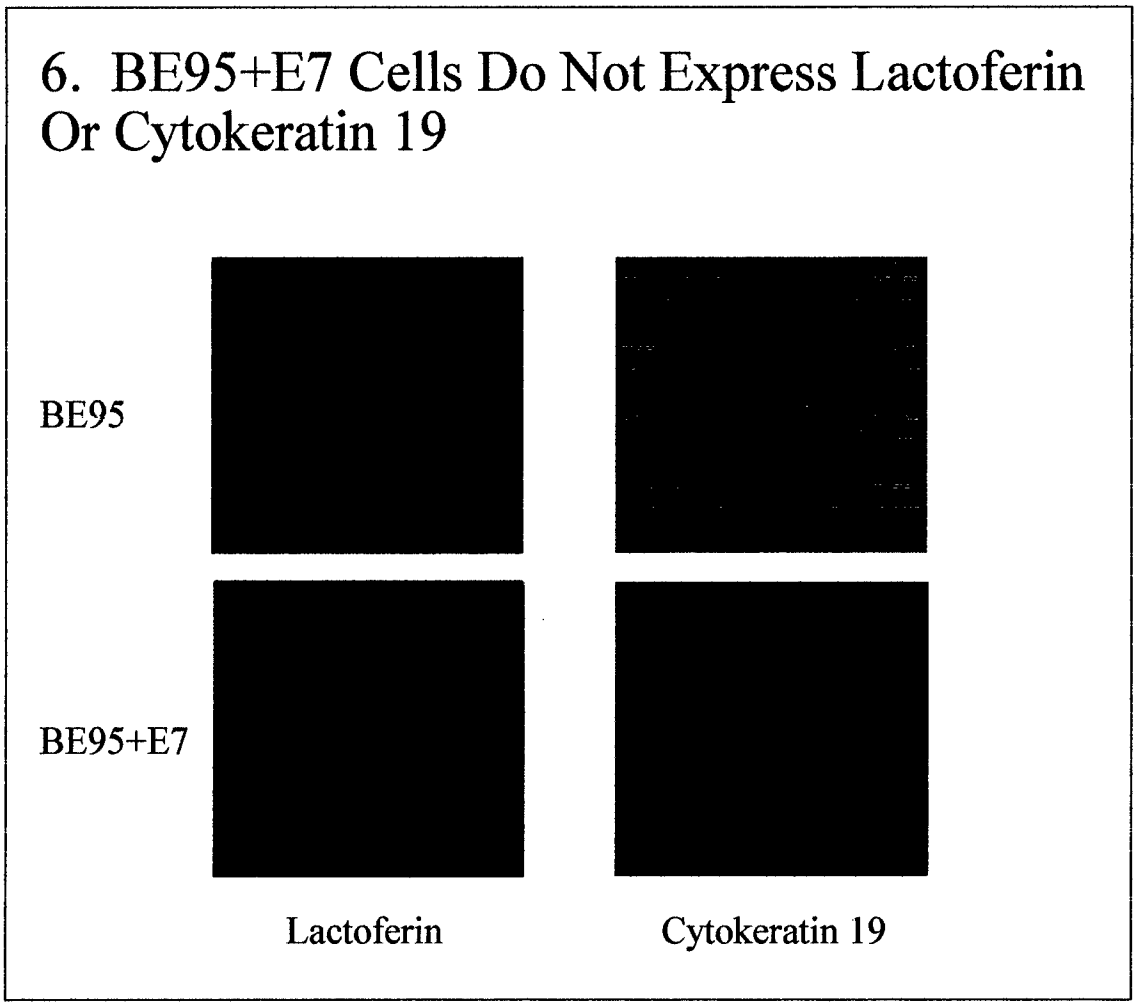

Figure 16. In contrast to BE95 spheroids, BE95+E7 spheroids did not express lactoferin or cytokeratin 19. In this experiment, cells were double stained for both proteins so for each cell line, the same spheroid is pictured in both panels. Most normal BE95 spheroids express the iron binding milk protein lactoferin in addition to the luminal differentiation marker cytokeratin 19. The BE95+E7 cells, however, do not appear to be expressing either of these proteins. Antibodies were used in the following concentrations: lactoferin (rabbit sera) 1:50 (Zymed), cytokeratin 19 (mouse IgG1, RCK108) 1:100 (DAKO), goat anti-rabbit-Texas Red 1:200 (Accurate Chemical and Scientific), and goat anti-mouse IgG1-fluorescein isothiocyanate 1:200 (Southern Biotechnology Associates).

Figure 17.

a. Conditionally inducible vectors.
To test the efficacy of the tetracycline regulated retroviral vector system, dominant-negative b-catenin genes were cloned into pRetro Off, pRetro On, and LINX. Following packaging, transfection into primary human mammary epithelial cells and two weeks of selection, total cell extracts were subjected to Western analysis using anti-C-terminal β-catenin antibody. As shown here, cells infected with pRetro ON construct did not induce dominant β-catenin at all. Cells infected with pRetro OFF induced dominant β-catenin in response to DOX removal, however the amount induced (shown as exogeneous) were much less than that of endogeneous protein. On the other hand, cells infected with LINX vector construct produced great response in both inducibility and amount.

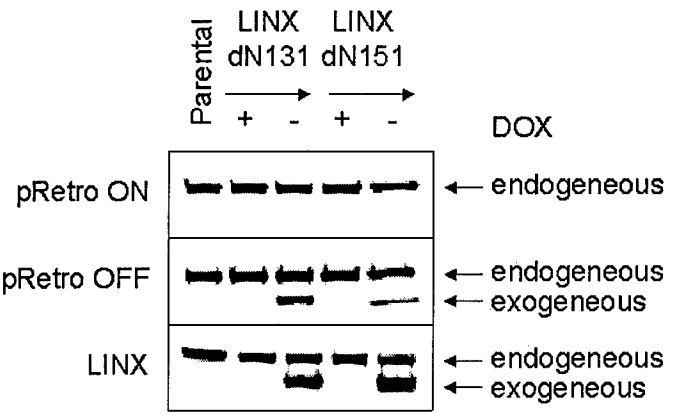

b. LEF1-Luciferase Reporter Assay.
Shown here are relative LEF1-reporter activities indicating that induced dominant β-catenin is in fact functional in regard to activating genes containing LEF1 responsive element.

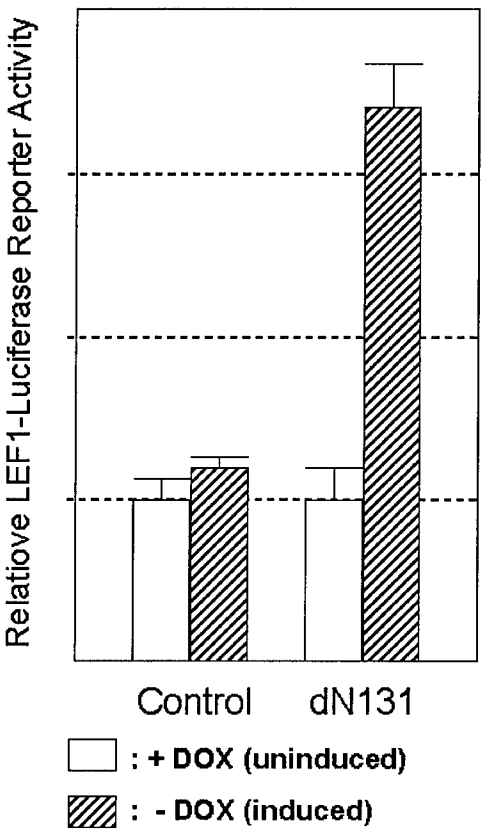

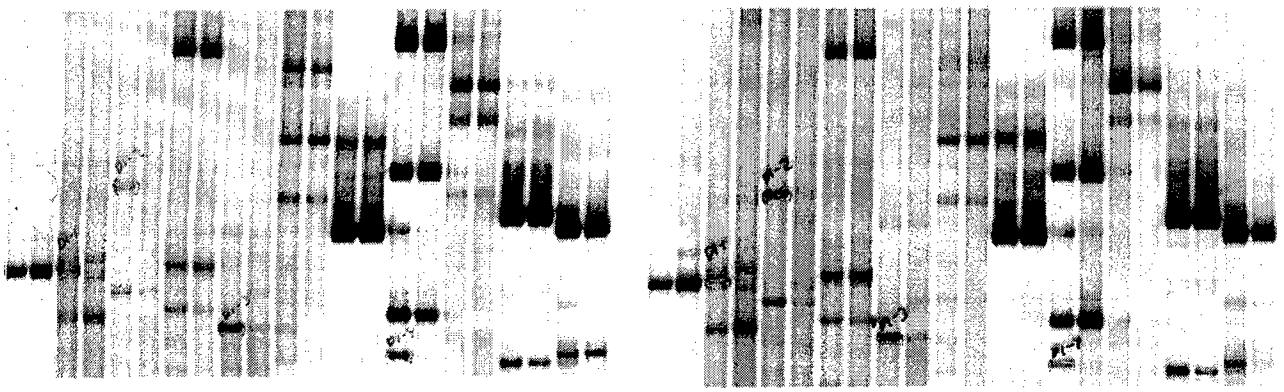

Figure 18. Differential Display Gel. This figure shows eleven paired normal and polyp samples tested with the Differential Display system. An RT-PCR product marked by the white arrow was recovered from the gel and identified as the differentially expressed gene CGM2. Also note the high degree of the high level of identity between paired lanes and between the two independent PCR preparations represented in the left and right panels.

Figure 19. RNase Protection Assay of CGM2. To confirm the differential expression level of genes identified using the Differential Display system, we compared the expression levels from normal crypt cells (N), adenomatous polyp cells (P) and carcinoma cells (C). A band indicating that the CGM2 gene is expressed only in normal crypt cells and not in the polyp or cancer cells is indicated by the black arrow.

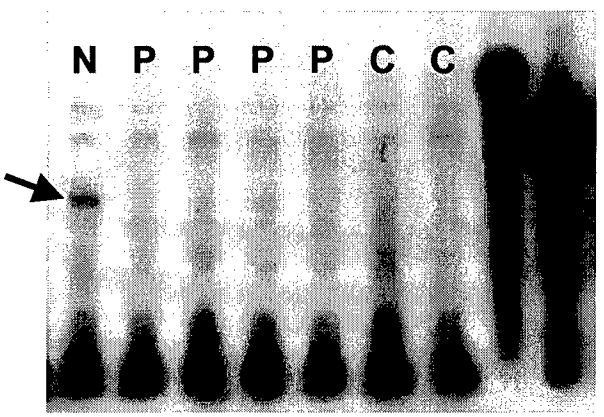

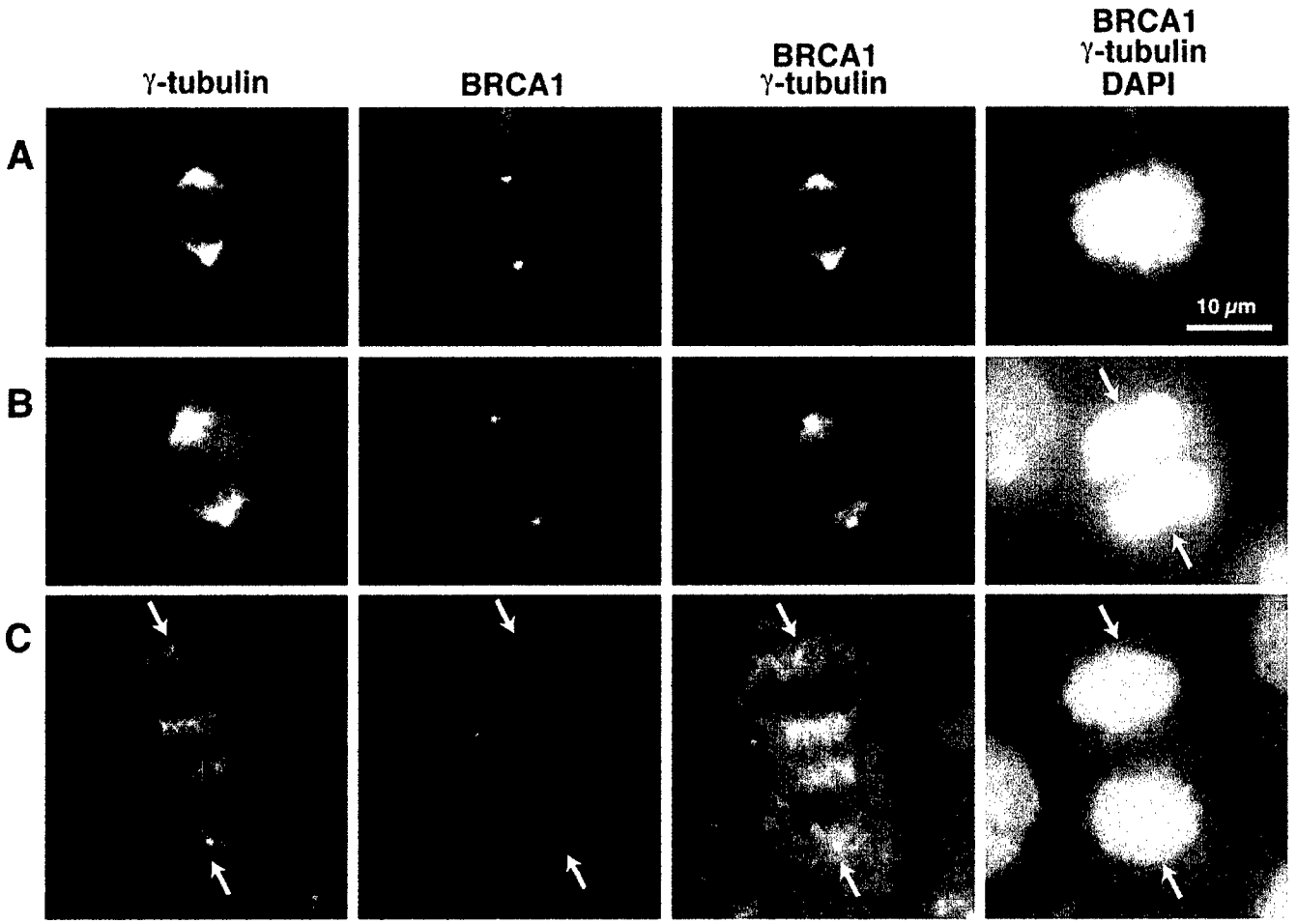

Figure 20. Coimmunostaining of COS-7 cells with mouse monoclonal γ-tubulin antibody and rabbit polyclonal BRCA1 antibody C-20. (A) A prometaphase to metaphase cell; (B) an early anaphase cell, and (C) a late anaphase cell. The colocalized signals of BRCA1 and γ-tubulin are yellow. DAPI counterstained DNA. Arrows indicate the positions of centrosomes.

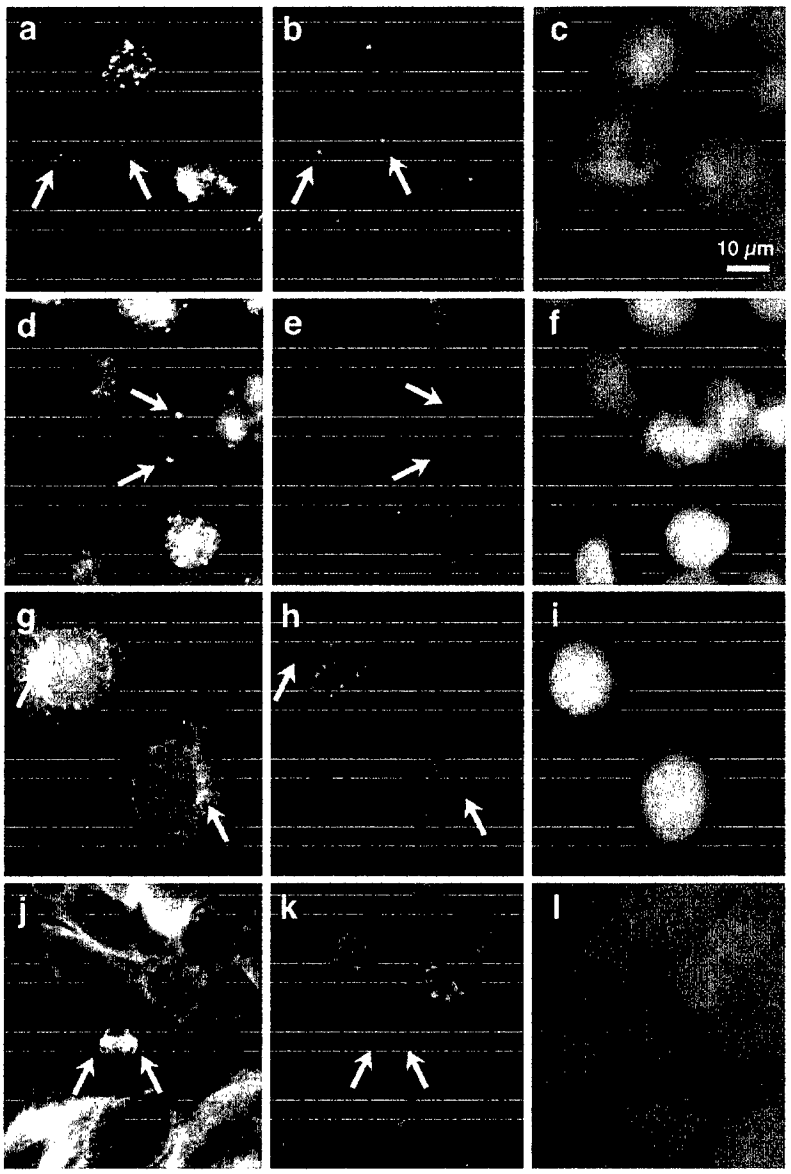

Figure 21. Immunostaining of COS-7 and E6/BE46 cells. Cells were costained with mouse monoclonal BRCA1 antibody MS110 (a) and rabbit polyclonal pericentrin antibody 4B (b); with MS110 (d) and rabbit polyclonal BRCA1 antibody C-20 (e); with mouse monoclonal γ-tubulin antibody (g) and C-20 (h); or with mouse monoclonal α-tubulin antibody (j) and C-20 (k). c, f, i, and l include DAPI counterstain of DNA. a-f highlight mitotic COS-7 cells; g-i are interphase COS-7 cells; j-l illustrate a mitotic E6/BE46 cell. Arrows indicate the positions of centrosomes.

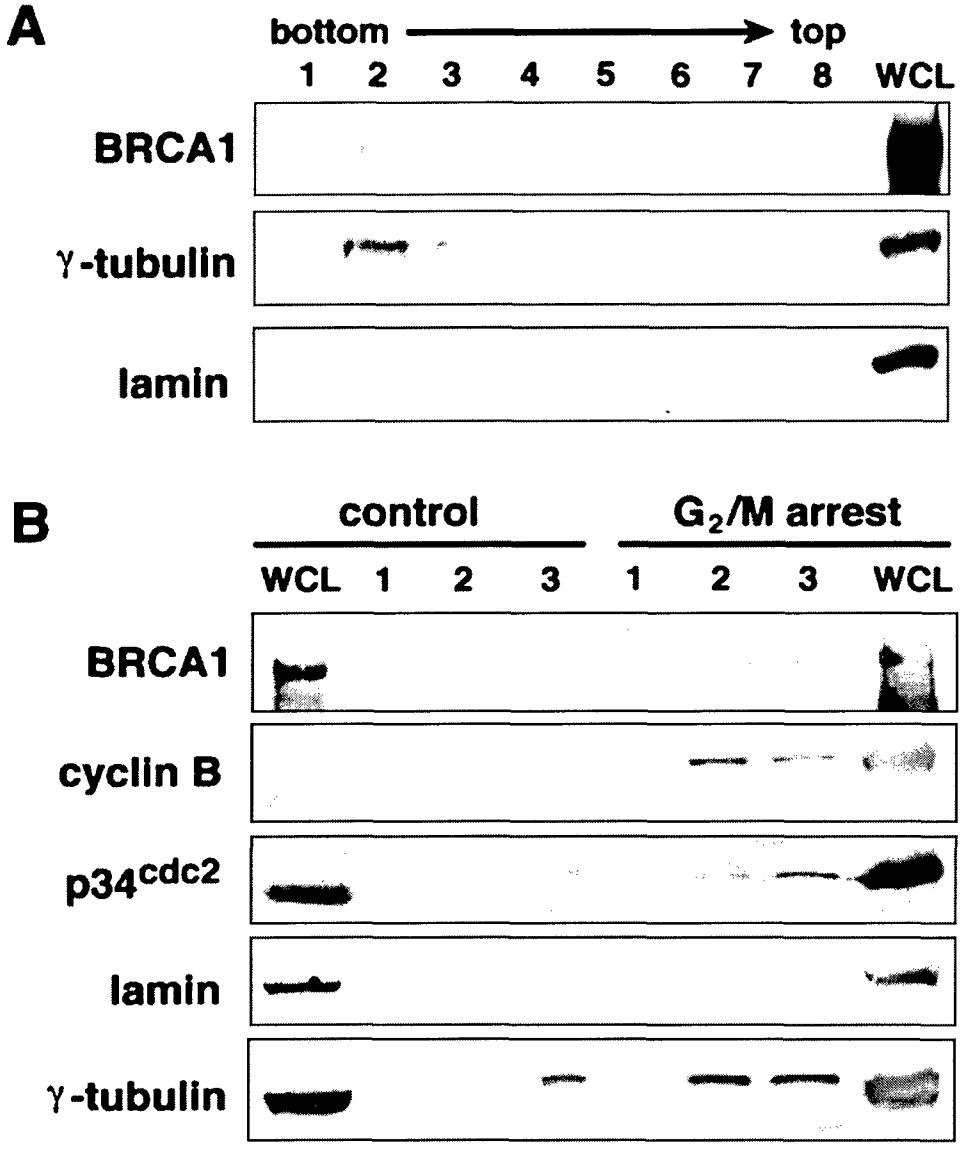

Figure 22. BRCA1 protein is detected in centrosome fractions purified by a discontinuous sucrose gradient. (A) COS-7 cells (1×10^7) were harvested in exponential growth phase. The proteins in each sucrose gradient fraction were separated by 4-15% gradient SDS/PAGE and subjected to Western blot analysis. (B) Approximately 5 × 106 of control COS-7 cells (cell cycle distribution: G0/G1, 37.21%; S, 45.15%; G2/M, 17.64%; CV, 6.25%) and cells arrested in G2/M by sequential treatment with thymidine and nocodazole (G0/G1, 5.51%; S, 36.60%; G2/M, 57.89%; CV, 8.69%) were used for centrosome preparations. Western blot analyses of fractions 1-3 of each sample are shown here. Whole-cell lysates were prepared from 2 × 105 cells. MS110 was used to detect BRCA1.

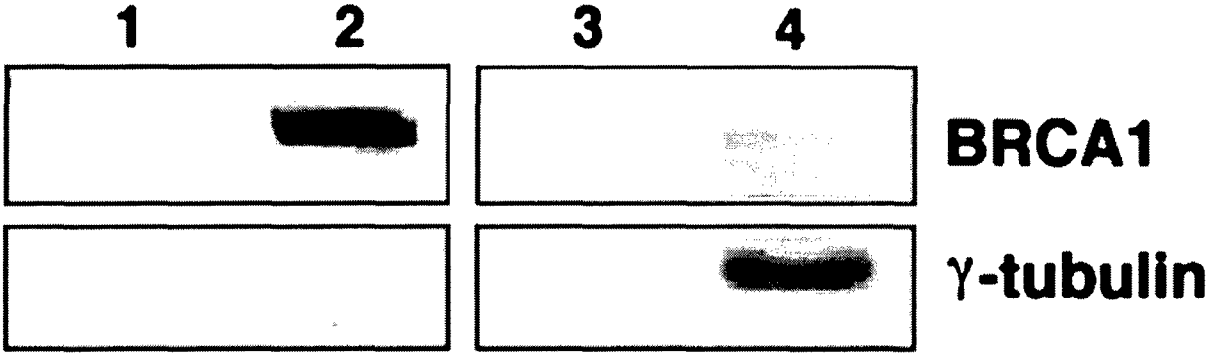

Figure 23. Coimmunoprecipitation of BRCA1 and γ-tubulin. Immunoprecipitation was performed by using rabbit polyclonal BRCA1 antibody C-20 (lane 2) or mouse monoclonal γ-tubulin antibody (lane 4), from 400 μg of COS-7 cell lysate. Normal rabbit IgG (lane 1) and mouse IgG (lane 3) were negative controls. Samples were separated by SDS/6% polyacrylamide gels and immunoblotted by BRCA1 MS110 and γ-tubulin antibody.

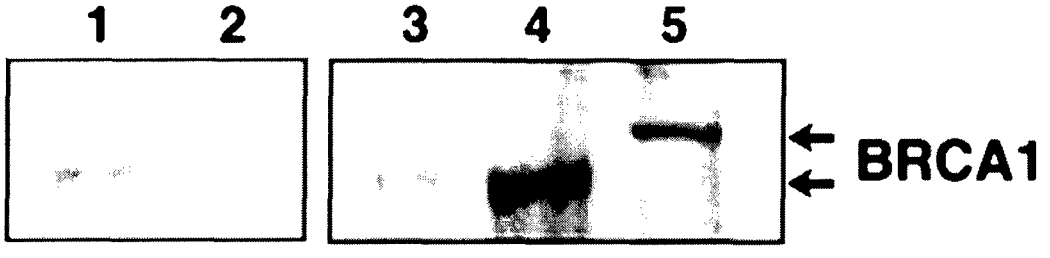

Figure 24. γ-tubulin associates preferentially with hypophosphorylated BRCA1. Samples were separated by 4-12% SDS/PAGE, and immunoblotted by BRCA1 MS110. Lane 1, isolated centrosomes; lanes 2 and 3, in vitro transcription/translation product of full-length BRCA1; lane 4, immunoprecipitation by γ-tubulin antibody; and lane 5, immunoprecipitation by C-20.

List of Salaried Personnel:

Name:	Position:
Nori Matsunami	Research Assistant professor
Leslie Jerominski	Research Associate
Ray White	P.I., Professor